

---

# Cavity Induced Many-body Polaritons: diamagnetic interactions, localization and coherent transfer

V. Rokaj<sup>1, 2\*</sup>, S. I. Mistakidis<sup>1, 2</sup> and H. R. Sadeghpour<sup>1</sup>

<sup>1</sup> ITAMP, Center for Astrophysics | Harvard & Smithsonian, Cambridge, Massachusetts 02138, USA

<sup>2</sup> Department of Physics, Harvard University, Cambridge, Massachusetts 02138, USA

\* vasil.rokaj@cfa.harvard.edu

July 8, 2022

## Abstract

Cavity quantum electrodynamics provides an ideal platform to engineer and control light-matter interactions with polariton quasiparticles. In this work, we investigate a many-body system of interacting particles in a harmonic trap coupled to a homogeneous quantum cavity field. The many-body system couples collectively to the cavity field, through its center of mass, and collective polariton states emerge. Due to the collective coupling, the cavity field mediates pairwise dipole-dipole interactions and enhances the effective mass of the particles. This leads to the localization of the center of mass which becomes maximal when light and matter are on resonance. The light-matter interaction modifies also the photonic properties of the system and the polariton ground state is populated with virtual, thermal (bunched) photons. In addition, the necessity of the diamagnetic  $A^2$  term for the stability of the many-body system is discussed, as in its absence a superradiant ground state instability occurs. We demonstrate the emergence of coherent transfer of polaritonic population under an external magnetic field by monitoring the underlying Landau-Zener probability.

---

## Contents

<b>1 Introduction</b>	<b>2</b>
<b>2 Many-Body System in a Cavity</b>	<b>4</b>
2.1 Kinematics of decoupling of center of mass and relative coordinates	5
<b>3 Many-Body Polariton States</b>	<b>6</b>
3.1 Derivation of the polariton states	7
3.2 Tunability of the polariton branches and limiting cases	8
3.3 Light-matter coupling regimes and polariton behavior	9
<b>4 Cavity Induced Localization and Resonance Effect</b>	<b>11</b>
4.1 Effective mass increase and resonance effect	13
<b>5 Cavity Induced Effective Matter Hamiltonian</b>	<b>14</b>

---

<b>6</b>	<b>Photon Occupations &amp; Photon Correlations</b>	<b>14</b>
6.1	Photon occupations & two-photon processes	15
6.2	Photon correlations	16
<b>7</b>	<b>Superradiant Instability</b>	<b>18</b>
<b>8</b>	<b>Polariton-Control with a Weak Magnetic Field</b>	<b>19</b>
8.1	Behavior of the polariton gap	21
8.2	Landau-Zener transition	22
<b>9</b>	<b>Summary and Outlook</b>	<b>23</b>
<b>A</b>	<b>Exact Solution in Free Space</b>	<b>25</b>
<b>B</b>	<b>Matter and Photon Operators in Terms of the Polaritonic Operators</b>	<b>26</b>
B.1	Photonic operators	26
B.2	Matter operators	27
<b>C</b>	<b>Computation of the Four-Point Photon Function</b>	<b>28</b>
	<b>References</b>	<b>29</b>

---

## 1 Introduction

Cavity quantum electrodynamics (cQED) is a rapidly evolving field, combining several different platforms for the manipulation and control of quantum matter with the aid of electromagnetic fields [1–3]. Its range of applicability spans from quantum optics [4], to polaritonic chemistry [5–13], as well as to ultra-cold gases in cavities [14], and light-induced states of matter using either classical [15, 16] or quantum cavity fields [17–20]. In the last decade, there has been an intense interest towards strong and ultrastrong light-matter interactions [21, 22], where light and matter entangle forming hybrid quasiparticle states known as polaritons [21, 23, 24].

Polaritons exhibit remarkable properties which have been probed in condensed matter [2], chemistry [1, 3, 25] and cold-atom [14] settings. Polaritons can lead, for instance, to modifications of chemical reactions [5, 7–12, 26], and to the control of excitons while also exciton-polariton condensation has been achieved [27–30]. Moreover, it has been suggested that strong light-matter interactions can influence the electron-phonon coupling and the critical temperature of superconductors [31–35]. Implications for coupling to chiral electromagnetic fields are currently under investigation [17, 36–39], and cavity-induced ferroelectric phases have been proposed [40, 41]. Landau levels in quantum Hall systems have demonstrated ultrastrong coupling to the cavity field [42–48] and Landau polariton states have been observed [42–44, 49, 50]. More recently, theoretical mechanisms on how to modify the integer Hall effect via the cavity field were proposed [51, 52] and the breakdown of the topological protection of the integer Hall effect due to the cavity was demonstrated experimentally [53].

All these exciting developments call for the further investigations on the properties of many-

body systems strongly coupled to the quantized cavity field. In this context, first-principle approaches have been put forward, such as the exact density-functional reformulation of QED [54–56], hybrid-orbital approaches [57], or generalized coupled cluster theory for analyzing polaritonic phenomena arising in light-matter systems [58, 59]. Complementary, analytical methods and exactly solvable models have played an important role in the development of many-body physics [60], and are highly desirable in the framework of cQED for understanding the origin of the microscopic mechanisms and induced phenomena of strongly correlated light-matter systems. Some of the key questions in this field include the polariton formation in many-body systems, the induced interactions in the matter subsystem due to the light field, the matter-mediated correlations between photons, as well as the control of polaritons with external probes [2, 3, 25].

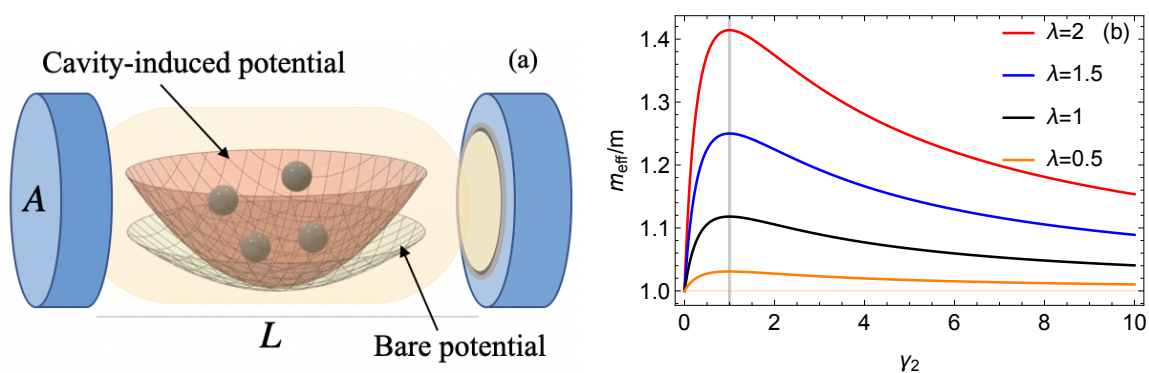


Figure 1: (a) Schematic representation of the interacting many-body system confined in the harmonic potential with frequency  $\Omega$  (bare potential in cyan) inside the cavity. The cavity field is considered homogeneous (depicted in light yellow), the area of the cavity mirrors is  $A$ , the distance among the mirrors is  $L$  and the fundamental cavity frequency  $\omega = \pi c/L$ . The impact of the cavity to the matter field can be effectively understood as a modified (in frequency) harmonic trap and the induction of pairwise dipole-dipole interactions. (b) Effective mass ratio  $m_{\text{eff}}/m$  as a function of the relative cavity frequency  $\gamma_2 = \omega/\Omega$  for different values of the light-matter coupling  $\lambda$ . Strikingly, the effective mass increases with respect to  $\gamma_2$ , it maximizes at resonance  $\gamma_2 = 1$  and for  $\gamma_2 > 1$  it decreases reaching asymptotically its original value,  $m_{\text{eff}} \rightarrow m$  for  $\gamma_2 \rightarrow \infty$ .

To address the above questions and provide analytical insights into light-matter correlated phenomena, we study a many-body system where the formation and properties of many-body polariton states can be obtained analytically. As depicted in Fig. 1(a) our system consists of  $N$  interacting particles in a harmonic trap embedded in a cavity, whose quantized field is treated in the long-wavelength limit [4, 61, 62]. The particles are considered to be structureless rendering our model exact for electrons, but also applicable to trapped cold ions, being effectively treated as having no internal structure [63]. Importantly, we showcase that due to the homogeneity of the cavity field in the long-wavelength limit, the light-matter correlations are solely associated with the center of mass (CM) of the particles.

The ground state properties of the light-matter system are studied thoroughly and we find that the polariton ground state contains virtual photons [64] which obey super-Poissonian statistics and are thus of thermal character, i.e., they bunch [65–67]. Further, we show that the cavity field enhances the localization of the CM wavefunction which is a consequence of the increasing

effective mass of the matter system. This localization phenomenon becomes maximal when the matter and cavity excitations are on resonance, as it can also be inferred from the effective mass in Fig. 1(b). In another context, this finding, could potentially provide insights on the resonance effect in polaritonic chemistry [5–7, 25, 68, 69]. In addition, we demonstrate that the cavity induced localization can be understood in terms of an effective Hamiltonian, describing solely the matter degrees of freedom, where the particles interact through a cavity induced potential [see Fig. 1(a)]. This description is expected to facilitate future many-body treatments avoiding the complication of explicitly using photon states.

The largely ignored diamagnetic  $\mathbf{A}^2$  term prevents the system from developing a superradiant instability. The latter refers to the situation where the ground state becomes unstable and the photon occupation diverges [70, 71]. It is also found that the many-body polariton states can be controlled with the use of a weak external magnetic field. In particular, there is an efficient inter-polariton exchange of energy and control of the polariton gap which is minimized away from the resonant point. This directly impacts the probability of the relevant Landau-Zener transition [72], which increases when the light and matter excitations are out of resonance.

This work proceeds as follows. Sec. 2 introduces the many-body model coupled to the cavity and demonstrates the separation of the relative coordinates from the cavity field. In Sec. 3 the exact solution for the many-body polariton states is outlined. Sec. 4 demonstrates the cavity induced localization and the resonance dependence of the effective mass. In Sec. 5 we derive the cavity mediated interactions and the effective matter Hamiltonian. Sec. 6 discusses the photonic properties of the polariton ground state, while in Sec. 7 we argue on the importance of the diamagnetic interactions regarding the stability of the system. The impact of a weak external magnetic field on the polariton states is appreciated in Sec. 8. In Sec. 9 we draw our conclusions and provide future perspectives. In Appendix A the exact solution in free space is presented, and in Appendices B and C details of several analytical computations are provided.

## 2 Many-Body System in a Cavity

We consider a system of  $N$  interacting particles, confined in a harmonic potential and coupled to the quantized cavity field. Such a system in the non-relativistic limit is described by the minimal-coupling Hamiltonian [1, 4, 73]

$$\hat{H} = \frac{1}{2m} \sum_{i=1}^N (\mathbf{i}\hbar\nabla_i + g_0\hat{\mathbf{A}})^2 + \sum_{i<l}^N W(|\mathbf{r}_i - \mathbf{r}_l|) + \sum_{i=1}^N \frac{m\Omega^2}{2} \mathbf{r}_i^2 + \sum_{\boldsymbol{\kappa}, \nu} \hbar\omega(\boldsymbol{\kappa}) \left( \hat{a}_{\boldsymbol{\kappa}, \nu}^\dagger \hat{a}_{\boldsymbol{\kappa}, \nu} + \frac{1}{2} \right), \quad (1)$$

where  $g_0$  is the single-particle coupling parameter to the quantized field  $\hat{\mathbf{A}}$ . For charged particles,  $g_0$  is in units of the elementary charge,  $e$ . The quantized electromagnetic vector potential  $\hat{\mathbf{A}}$  in the long-wavelength limit (homogeneous approximation) reads [4, 22, 61, 73]

$$\hat{\mathbf{A}} = \sum_{\boldsymbol{\kappa}, \nu} \sqrt{\frac{\hbar}{2\epsilon_0 \mathcal{V} \omega(\boldsymbol{\kappa})}} \boldsymbol{\varepsilon}_\nu(\boldsymbol{\kappa}) \left( \hat{a}_{\boldsymbol{\kappa}, \nu} + \hat{a}_{\boldsymbol{\kappa}, \nu}^\dagger \right). \quad (2)$$

Here,  $\boldsymbol{\kappa} = (\kappa_x, \kappa_y, \kappa_z)$  are the wave vectors of the photon field,  $\omega(\boldsymbol{\kappa}) = c|\boldsymbol{\kappa}|$  are the allowed frequencies in the quantization volume  $\mathcal{V}$ ,  $\epsilon_0$  is the vacuum permittivity and  $\lambda = 1, 2$  denote the two transversal polarization directions [73, 74]. The polarization vectors satisfy  $\boldsymbol{\varepsilon}_\nu(\boldsymbol{\kappa}) \cdot \boldsymbol{\kappa} = 0 \quad \forall \boldsymbol{\kappa}$ , and can be taken to be mutually perpendicular  $\boldsymbol{\varepsilon}_\nu(\boldsymbol{\kappa}) \cdot \boldsymbol{\varepsilon}_{\nu'}(\boldsymbol{\kappa}) = \delta_{\nu\nu'}$ . The operators  $\hat{a}_{\boldsymbol{\kappa}, \nu}$  and  $\hat{a}_{\boldsymbol{\kappa}, \nu}^\dagger$

are the annihilation and creation operators of the photon field obeying  $[\hat{a}_{\kappa,\nu}, \hat{a}_{\kappa',\nu'}^\dagger] = \delta_{\kappa\kappa'} \delta_{\nu\nu'}$ . The photon operators can also be defined in terms of the displacement coordinates  $q_{\kappa,\nu}$  and their conjugate momenta  $\partial/\partial q_{\kappa,\nu}$  as [73, 75]

$$\hat{a}_{\kappa,\nu} = \frac{1}{\sqrt{2}} \left( q_{\kappa,\nu} + \frac{\partial}{\partial q_{\kappa,\nu}} \right) \quad (3)$$

and  $\hat{a}_{\kappa,\nu}^\dagger$  defined by conjugation.

## 2.1 Kinematics of decoupling of center of mass and relative coordinates

The covariant kinetic energy term through which the light-matter coupling and correlations enter has the following form,

$$-\hbar^2 \sum_{i=1}^N \nabla_i^2 + 2ig_0 \hbar \hat{\mathbf{A}} \cdot \sum_{i=1}^N \nabla_i + Ng_0^2 \hat{\mathbf{A}}^2. \quad (4)$$

The quantized field couples to the total momentum, implying that the CM couples collectively to the cavity field, because the field is homogeneous. Consequently, it is beneficial to transform the Hamiltonian into the CM frame and relative coordinates for describing properly the matter-photon interaction and correlations. Namely

$$\mathbf{R} = \frac{1}{\sqrt{N}} \sum_{i=1}^N \mathbf{r}_i \quad \text{and} \quad \mathbf{R}_j = \frac{\mathbf{r}_1 - \mathbf{r}_j}{\sqrt{N}} \quad \text{for } j > 1. \quad (5)$$

As expected, the respective relative and CM conjugate operators commute, demonstrating the independence of position and momentum coordinates<sup>1</sup>. In the new coordinates, the cavity field couples only to the CM momentum,

$$\hat{\mathbf{A}} \cdot \sum_{i=1}^N \nabla_i = \sqrt{N} \hat{\mathbf{A}} \cdot \nabla_{\mathbf{R}}, \quad (6)$$

whose scaling with  $\sqrt{N}$  should be expected. The scalar trapping potential also separates into two independent parts, one depending on the CM coordinate and one depending on the relative coordinates, without any crossing terms between  $\mathbf{R}$  and  $\mathbf{R}_j$ , i.e.

$$\sum_{i=1}^N \mathbf{r}_i^2 = \mathbf{R}^2 + N \sum_{j=2}^N \mathbf{R}_j^2 - \left( \sum_{j=2}^N \mathbf{R}_j \right)^2. \quad (7)$$

The two-body interaction between the particles depends only on the relative coordinates, i.e.

$$\sum_{i<l}^N W(|\mathbf{r}_i - \mathbf{r}_l|) = \sum_{1<l}^N W(\sqrt{N}|\mathbf{R}_l|) + \sum_{2 \leq i < l}^N W(\sqrt{N}|\mathbf{R}_i - \mathbf{R}_l|), \quad (8)$$

<sup>1</sup>A model of electrons in cavity was recently considered in [76], where a separation of the relative coordinates from the CM and the cavity field was formulated. However, as it was also stated in Ref. [76], the coordinates are linearly dependent and thus the separation of coordinates is not achieved.

and thereby does not affect the cavity-induced CM motion. The Hamiltonian therefore has two parts: (i) the CM contribution via  $\hat{H}_{\text{cm}}$  which couples to the quantized field  $\hat{\mathbf{A}}$  and (ii) the relative contribution  $\hat{H}_{\text{rel}}$  being decoupled from both the cavity field  $\hat{\mathbf{A}}$  and the CM. As such,  $\hat{H} = \hat{H}_{\text{cm}} + \hat{H}_{\text{rel}}$ , where

$$\begin{aligned}\hat{H}_{\text{cm}} &= \frac{1}{2m} (\mathbf{i}\hbar\nabla_{\mathbf{R}} + g_0\sqrt{N}\hat{\mathbf{A}})^2 + \frac{m\Omega^2}{2}\mathbf{R}^2 + \sum_{\kappa,\nu} \hbar\omega(\kappa) \left( \hat{a}_{\kappa,\nu}^\dagger \hat{a}_{\kappa,\nu} + \frac{1}{2} \right), \\ \hat{H}_{\text{rel}} &= \frac{1}{2m} \sum_{j=2}^N \left( \frac{\mathbf{i}\hbar}{\sqrt{N}} \nabla_{\mathbf{R}_j} \right)^2 - \frac{\hbar^2}{2mN} \sum_{j,k=2}^N \nabla_{\mathbf{R}_j} \cdot \nabla_{\mathbf{R}_k} + \frac{m\Omega^2}{2} N \sum_{j=2}^N \mathbf{R}_j^2 - \frac{m\Omega^2}{2} \left( \sum_{j=2}^N \mathbf{R}_j \right)^2 \\ &\quad + \sum_{1<l}^N W(\sqrt{N}|\mathbf{R}_l|) + \sum_{2\leq i<l}^N W(\sqrt{N}|\mathbf{R}_i - \mathbf{R}_l|).\end{aligned}\tag{9}$$

Therefore, it has been demonstrated that for a homogeneous cavity field and harmonically trapped particles, the light-matter interaction takes place between the cavity field and the CM. The pairwise interaction drops out because our treatment of many-body system is for structureless particles coupled to a homogeneous cavity field. This is a generalization of Kohn's theorem [77] which for a homogeneous electron gas in a homogeneous magnetic field, produces CM cyclotron transitions unaffected by two-body interactions. While inhomogeneous light or anharmonic trapping potentials couple the relative motion to the cavity, in a further publication, we will elucidate for atomic systems, that pair interactions will intuitively couple to the cavity [78]. It is important to note, that our demonstration of the decoupling of the two-body interaction from the light-matter part holds for an arbitrary number of quantized modes, as long as they are still considered in the (homogeneous) long-wavelength limit. In addition, the decoupling of the relative coordinates from the CM and the cavity field holds for an external homogeneous time-dependent classical field  $\mathbf{A}_{\text{ext}}(t)$ ,  $\mathbf{E}_{\text{ext}}(t) = -\partial_t \mathbf{A}_{\text{ext}}(t)$ .

### 3 Many-Body Polariton States

We consider now the case of a single-mode cavity, i. e.,  $\kappa_x = \kappa_y = 0$  while  $\kappa_z \neq 0$ . Then, the polarization vectors are  $\boldsymbol{\varepsilon}_1 = \mathbf{e}_x$  and  $\boldsymbol{\varepsilon}_2 = \mathbf{e}_y$  and the field simplifies to

$$\hat{\mathbf{A}} = \sum_{\nu=x,y} \sqrt{\frac{\hbar}{2\epsilon_0\mathcal{V}\omega}} \mathbf{e}_\nu (\hat{a}_\nu + \hat{a}_\nu^\dagger).\tag{10}$$

The light-matter Hamiltonian then takes the form of a system of interacting harmonic oscillators

$$\hat{H}_{\text{cm}} = -\frac{\hbar^2}{2m} \nabla_{\mathbf{R}}^2 + \frac{ig_0\hbar}{m} \sqrt{N}\hat{\mathbf{A}} \cdot \nabla_{\mathbf{R}} + \frac{m\Omega^2}{2}\mathbf{R}^2 + \underbrace{\frac{Ne^2}{2m}\hat{\mathbf{A}}^2 + \sum_{\nu=x,y} \hbar\omega \left( \hat{a}_\nu^\dagger \hat{a}_\nu + \frac{1}{2} \right)}_{\hat{H}_p},\tag{11}$$

where  $\hat{H}_p$  denotes the purely photonic Hamiltonian. The photonic part  $\hat{H}_p$  can be brought to the diagonal form of a harmonic oscillator through the scaling transformation  $u_\nu = q_\nu \sqrt{\tilde{\omega}/\omega}$  [see Eq. (3) for the definition of  $q_\nu$  in terms of  $\hat{a}_\nu$  and  $\hat{a}_\nu^\dagger$ ] on the photonic displacement coordinates [50] and becomes  $\hat{H}_p = \sum_\nu \frac{\hbar\tilde{\omega}}{2} (-\partial^2/\partial u_\nu^2 + u_\nu^2)$ . The frequency  $\tilde{\omega}$  is the dressed cavity frequency

$$\tilde{\omega} = \sqrt{\omega^2 + \omega_d^2}\tag{12}$$

that depends on the *diamagnetic frequency*  $\omega_d$

$$\omega_d = \sqrt{\frac{g_0^2 N}{m\epsilon_0 \mathcal{V}}} = \sqrt{\frac{e^2 n_{2D} \omega}{m\epsilon_0 \pi c}}. \quad (13)$$

The latter originates from the collective coupling of the particles to the transversal quantized field and is due to the  $\hat{\mathbf{A}}^2$  term in the Hamiltonian [50, 61, 62, 79–81]. Note that in Eq. (13), we used the expression for the fundamental cavity frequency  $\omega = \pi c/L$  and we introduced the 2D particle density  $n_{2D} = N/A$ , where  $A$  refers to the area of the cavity mirrors and  $L$  to the cavity length as shown in Fig. 1(a).

### 3.1 Derivation of the polariton states

After the scaling transformation the full CM Hamiltonian reads

$$\hat{H}_{\text{cm}} = \sum_{\nu=x,y} \left[ -\frac{\hbar^2}{2m} \frac{\partial^2}{\partial R_\nu^2} + \frac{m\Omega^2 R_\nu^2}{2} + ig\sqrt{2}u_\nu \frac{\partial}{\partial R_\nu} + \frac{\hbar\tilde{\omega}}{2} \left( -\frac{\partial^2}{\partial u_\nu^2} + u_\nu^2 \right) \right] \equiv \sum_{\nu=x,y} \hat{H}_\nu. \quad (14)$$

From the above it is clear that the Hamiltonian of our system consists of two copies, namely  $\hat{H}_{\text{cm}} = \sum_\nu \hat{H}_\nu$ , representing two interacting harmonic oscillators. Therefore, without loss of generality, since the field is the same along both spatial directions, we focus on a single copy, i.e.  $\hat{H}_\nu$ . To avoid any confusion we note that  $\mathbf{R} = (R_x, R_y) = (X, Y)$  and  $\nabla = (\partial_x, \partial_y)$ . Further, in Eq. (14) we introduced the collective light-matter coupling constant  $g = \omega_d \sqrt{\hbar^3/2m\tilde{\omega}}$  which depends on the particle number  $N$  through the diamagnetic frequency  $\omega_d$ . Notice that the scaling  $g \sim \sqrt{N}$  is the same with the standard behavior of the collective light-matter coupling utilized in the few-level models of quantum optics [21, 82–84] and it is a consequence of having a collective excitation (of the CM) that couples to the cavity.

Importantly, the coupling term between the two oscillators is between the coordinate  $u_\nu$  and the momentum  $\partial/\partial R_\nu$ . Performing the Fourier transform,  $\phi(R_\nu) = \int_{-\infty}^{\infty} \frac{dK_\nu}{2\pi} \tilde{\phi}(K_\nu) e^{iK_\nu R_\nu}$  it can be brought into the form of a coordinate-coordinate coupling term, which is much easier to handle analytically. This way, it becomes

$$\hat{H}_\nu = -\frac{m\Omega^2}{2} \frac{\partial^2}{\partial K_\nu} + \frac{\hbar^2}{2m} K_\nu^2 - g\sqrt{2}K_\nu u_\nu + \frac{\hbar\tilde{\omega}}{2} \left[ -\frac{\partial^2}{\partial u_\nu^2} + u_\nu^2 \right]. \quad (15)$$

A more detailed discussion on the Fourier transform of a quantum harmonic oscillator can be found in Ref. [85]. It is convenient to introduce the scaled coordinates  $V_{\nu+} = K_\nu \sqrt{\hbar^2/m\Omega^2}$  and  $V_{\nu-} = -u_\nu \sqrt{\hbar/\tilde{\omega}}$  in order to bring the Hamiltonian into the form of two interacting harmonic oscillators with unit mass

$$\hat{H}_\nu = -\frac{\hbar^2}{2} \sum_{l=\pm} \frac{\partial^2}{\partial V_{\nu l}^2} + \frac{1}{2} \sum_{l,j=\pm} W_{lj} V_{\nu l} V_{\nu j}, \quad (16)$$

where the elements of  $W$  are  $W_{++} = \Omega^2$ ,  $W_{--} = \tilde{\omega}^2$  and  $W_{+-} = W_{-+} = \omega_d \Omega$  and thus the matrix  $W$  is real and symmetric. As a consequence it can be diagonalized by the orthogonal matrix  $O$  [62],

$$O = \begin{pmatrix} \frac{1}{\sqrt{1+\Lambda^2}} & \frac{\Lambda}{\sqrt{1+\Lambda^2}} \\ -\frac{\Lambda}{\sqrt{1+\Lambda^2}} & \frac{1}{\sqrt{1+\Lambda^2}} \end{pmatrix} \text{ with } \Lambda = \alpha - \sqrt{1+\alpha^2}$$

and  $\alpha = (\Omega^2 - \tilde{\omega}^2)/2\omega_d\Omega$ . It can be easily deduced that the parameter  $\Lambda$  quantifies how much the matrix  $O$  deviates from being diagonal. Additionally, the eigenvalues of the matrix  $W$  give the new normal modes (polariton branches) of the interacting light-matter system

$$\Omega_{\pm}^2 = \frac{1}{2} \left( \tilde{\omega}^2 + \Omega^2 \pm \sqrt{4\omega_d^2\Omega^2 + (\tilde{\omega}^2 - \Omega^2)^2} \right). \quad (17)$$

The Hamiltonian after the orthogonal transformation takes the canonical form

$$\hat{H}_\nu = -\frac{\hbar^2}{2} \sum_{l=\pm} \frac{\partial^2}{\partial S_{\nu l}^2} + \frac{1}{2} \sum_{l=\pm} \Omega_l^2 S_{\nu l}^2. \quad (18)$$

The new coordinates  $S_{\nu l}$  and conjugate momenta  $\partial_{S_{\nu l}}$  are related to the old ones  $\{V_{\nu l}, \partial_{V_{\nu l}}\}$  through the orthogonal matrix  $O$  [62],  $S_{\nu l} = \sum_j O_{jl} V_{\nu j}$  and  $\partial/\partial S_{\nu l} = \sum_j O_{jl} \partial/\partial V_{\nu j}$ . As it can be seen,  $\Lambda$  is the mixing parameter between the matter and the photonic degrees of freedom. Due to the fact that the matrix  $O$  is orthogonal the canonical commutation relations are satisfied which implies that we have two independent harmonic oscillators [62]. Thus, the polariton eigenfunctions of the system are Hermite functions  $\phi$  of coordinates  $S_{\nu+}$  and  $S_{\nu-}$

$$\Psi_{n_+, n_-}(S_{\nu+}, S_{\nu-}) = \phi_{n_+}(S_{\nu+}) \otimes \phi_{n_-}(S_{\nu-}), \quad n_{\pm} \in \mathbb{N} \quad (19)$$

with eigenspectrum

$$E_{n_+, n_-} = \hbar\Omega_+ \left( n_+ + \frac{1}{2} \right) + \hbar\Omega_- \left( n_- + \frac{1}{2} \right). \quad (20)$$

Moreover, it is useful to express the diagonalized Hamiltonian  $\hat{H}_{\text{cm}}$  in terms of polaritonic annihilation,  $\hat{d}_{\nu l} = S_{\nu l} \sqrt{\Omega_l/2\hbar} + \sqrt{\hbar/2\Omega_l} \partial_{S_{\nu l}}$ , and creation,  $\hat{d}_{\nu l}^\dagger = S_{\nu l} \sqrt{\Omega_l/2\hbar} - \sqrt{\hbar/2\Omega_l} \partial_{S_{\nu l}}$ , operators [75] namely

$$\hat{H}_\nu = \sum_{l=\pm} \hbar\Omega_l \left( \hat{d}_{\nu l}^\dagger \hat{d}_{\nu l} + \frac{1}{2} \right). \quad (21)$$

We note that the polariton eigenstates  $\Psi_{n_+, n_-}(S_{\nu+}, S_{\nu-})$  can also be written as Fock states  $\Psi_{n_+, n_-}(S_{\nu+}, S_{\nu-}) \equiv |n_+\rangle_\nu |n_-\rangle_\nu$ , which can be constructed by applying the polariton creation operators  $\hat{d}_{\nu+}^\dagger$  and  $\hat{d}_{\nu-}^\dagger$  on the polaritonic vacuum states  $|0_+\rangle_\nu$  and  $|0_-\rangle_\nu$  respectively [74, 75].

### 3.2 Tunability of the polariton branches and limiting cases

**Decoupling limit.** The light-matter interaction in our system is controlled by the diamagnetic frequency  $\omega_d$ . As  $\omega_d \rightarrow 0$  the polariton modes become  $\Omega_{\pm}^2 = \frac{1}{2} (\omega^2 + \Omega^2 \pm \sqrt{(\omega^2 - \Omega^2)^2})$ . When  $\Omega > \omega$ , the upper polariton branch tends to  $\Omega_+ \rightarrow \Omega$ , while the lower polariton approaches  $\Omega_- \rightarrow \omega$ . For  $\omega > \Omega$ , the situation is inverted, namely  $\Omega_+ \rightarrow \omega$  and  $\Omega_- \rightarrow \Omega$ . Thus, the correct decoupling limit is consistently recovered.

**No-trap limit.** Considering the situation in which the external trap vanishes, i.e.  $\Omega \rightarrow 0$ , we have freely-moving particles coupled to the cavity. In this limit, the upper (lower) polariton branch approaches the dressed cavity frequency (zero), namely  $\Omega_+ \rightarrow \tilde{\omega}$  ( $\Omega_- \rightarrow 0$ ). This is consistent with the free particle solution in the cavity, where there is only one discrete mode in the system,  $\tilde{\omega}$ , as it was demonstrated in Ref. [64]. The appearance of only one quantized mode means that in the no-trap limit, one part of the spectrum becomes continuous [64]. This is indeed the case here, see e.g. Appendix A, where we exactly solve the many-body system in the absence of the harmonic potential.



---

**Tuning parameters.** The polaritonic branches [Eq. (17)] are tunable through: (i) the particle number (or particle density) appearing in the diamagnetic frequency  $\omega_d$  and (ii) the cavity frequency  $\omega$  which can be varied by changing the distance  $L$  among the cavity mirrors. The normalized polariton modes in terms of the trap frequency  $\Omega$  read

$$\frac{\Omega_{\pm}}{\Omega} = \sqrt{\frac{\gamma_1^2 + \gamma_2^2 + 1 \pm \sqrt{4\gamma_1^2 + (\gamma_1^2 + \gamma_2^2 - 1)^2}}{2}}, \quad (22)$$

where  $\gamma_1 = \omega_d/\Omega$  and  $\gamma_2 = \omega/\Omega$  are dimensionless ratios. Notice also that the mixing parameter  $\Lambda = \alpha - \sqrt{1 + \alpha^2}$ , defined in Eq. (17), can be equivalently written solely in terms of  $\gamma_1$  and  $\gamma_2$  as  $\alpha = (\gamma_1^{-1} - \gamma_1 - \gamma_2^2 \gamma_1^{-1})/2$ . Notably, the dimensionless ratios are not independent because the diamagnetic frequency  $\omega_d$  is also a function of  $\omega$  [see Eq. (13)]. As a consequence, the normalized diamagnetic frequency  $\omega_d/\Omega$  can be written as

$$\gamma_1 = \frac{\omega_d}{\Omega} = \sqrt{\frac{g_0^2 N / Am \epsilon_0 \pi c}{\Omega}} \sqrt{\frac{\omega}{\Omega}} = \lambda \sqrt{\gamma_2}. \quad (23)$$

Thus, the two independent dimensionless parameters in our setting are

$$\lambda = \sqrt{\frac{g_0^2 N}{Am \epsilon_0 \pi c \Omega}} \quad \text{and} \quad \gamma_2 = \frac{\omega}{\Omega}. \quad (24)$$

From this expression becomes evident that the dimensionless light-matter coupling  $\lambda$  can be tuned by varying the particle number  $N$  and the area of the cavity mirrors  $A$ . Thus,  $\lambda$  can be flexibly adjusted taking a wide range of values which correspond to different light-matter coupling regimes.

### 3.3 Light-matter coupling regimes and polariton behavior

**Light-matter coupling regimes.** To set the stage for addressing the behavior of our polariton states we first briefly summarize the characteristics of the different light-matter interaction regimes. In the weak coupling regime the physics is dictated by the Purcell effect [86], where there is no hybridization between light and matter. While in the strong coupling hybridization enforces the emergence of the Rabi splitting. Experimentally, the two situations are understood by comparing the losses of the system to the light-matter coupling strength [21]. In contrast, the ultrastrong coupling regime is defined by the dimensionless ratio between the light-matter coupling strength and the bare excitations of the system [21]. Thus, this regime determines whether perturbation theory is applicable for the coupled system or whether particular approximations, such as the rotating-wave approximation can be used [21]. Typically, in this regime the Rabi split is comparable to the bare system excitations and the counter-rotating and the diamagnetic  $\mathbf{A}^2$  terms need to be included [21] as it has been demonstrated also experimentally [44]. Furthermore, the so-called deep strong coupling regime has also been achieved where the ratio between the light-matter coupling and the bare excitations approaches unity [42] or even goes beyond it [45]. We will now study the the influence of  $\lambda$  and  $\gamma_2$  on the polariton modes.

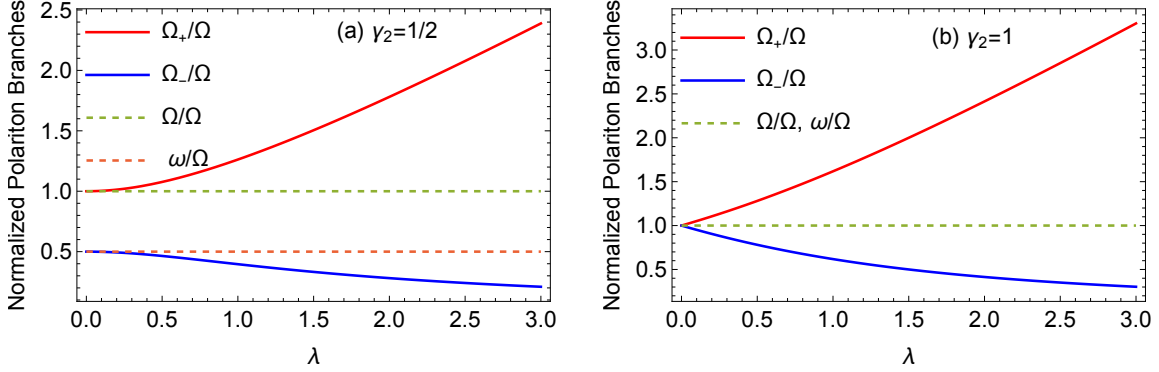


Figure 2: Normalized polariton branches  $\Omega_+/\Omega$  and  $\Omega_-/\Omega$  (solid lines) as a function of the light-matter coupling  $\lambda$ . In (a) the cavity and the harmonic trap are off-resonance with  $\gamma_2 = \omega/\Omega = 1/2$ , while in (b) they are in resonance i.e.  $\gamma_2 = \omega/\Omega = 1$ . The dashed lines indicate the bare excitation frequencies of the trap and the cavity. In both cases the polariton gap increases for larger  $\lambda$ .

**Polariton behavior.** Let us start by investigating the impact of the light-matter coupling,  $\lambda$  on the polariton branches. For simplicity, the cavity frequency  $\omega$  (or equivalently  $\gamma_2$ ) is held fixed. The resultant upper and lower polaritons as a function of  $\lambda$  are presented in Fig. 2 for two different values of the relative cavity frequency  $\gamma_2$ . The case of  $\gamma_2 = 1/2$  corresponding to the situation where the cavity frequency  $\omega$  is off-resonant with the trap frequency  $\Omega$  is depicted in Fig. 2(a). The upper polariton branch,  $\Omega_+$ , increases as function of  $\lambda$  while the lower one decreases approaching zero asymptotically. As expected, in the decoupling limit,  $\lambda \rightarrow 0$ , it holds that  $\Omega_+ \rightarrow \Omega$  and  $\Omega_- \rightarrow \omega$ . Moreover, we observe that the two polariton branches are always separated and do not coincide even for  $\lambda \rightarrow 0$  since the cavity and the trap frequencies are off-resonance ( $\omega \neq \Omega$ ). Considering a resonantly coupled cavity with the trap,  $\gamma_2 = 1$ , [Fig. 2(b)] it is found that  $\Omega_+$  increases and  $\Omega_-$  decreases as a function of  $\lambda$  but with a faster rate in comparison to the off-resonant situation. Due to the resonance condition the polariton gap closes for the light-matter interaction approaching zero,  $\lambda \rightarrow 0$ . It is important to mention that despite the fact that the lower polariton is “softer” and its value smaller than the upper polariton, the former is actually more important for the low energy physics of the system. This is especially the case in the ultrastrong and the deep strong coupling regimes since then the energy gap between the two polaritons will be filled with multiple of the excited states ( $n_- > 0$ ) of the lower polariton.

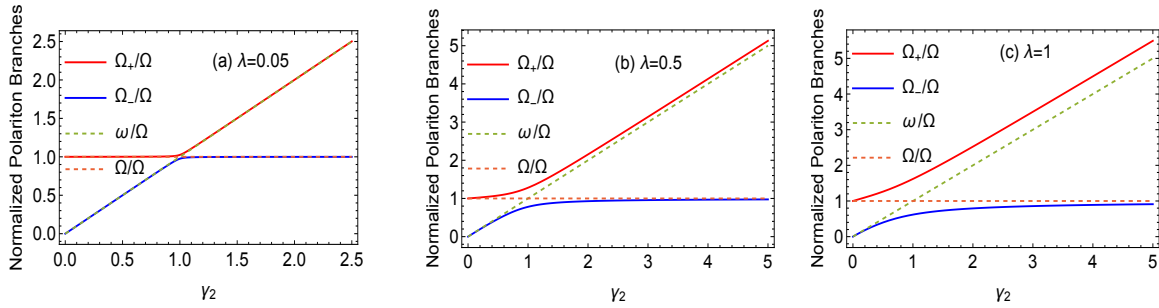


Figure 3: Normalized polariton branches  $\Omega_+/\Omega$  and  $\Omega_-/\Omega$  (solid lines) as a function of  $\gamma_2 = \omega/\Omega$  and fixed values of the light-matter coupling  $\lambda$  (see legends). Dashed lines mark the bare excitation frequencies of the matter and the cavity fields. In (a)  $\lambda = 0.05$  where an avoided crossing (Rabi splitting) appears at the resonance point  $\gamma_2 = 1$ . In (b)  $\lambda = 0.5$  with the Rabi splitting becoming comparable to the one of bare excitations implying ultrastrong coupling, while in (c)  $\lambda = 1$  we enter the deep strong coupling regime in which the upper polariton is parallel to the photon excitation without reaching it.

Next, we study the behavior of the polaritons as a function of the relative cavity frequency  $\gamma_2 = \omega/\Omega$  for different values of the light-matter interaction  $\lambda$ . Fig. 3(a) illustrates the normalized polariton branches  $\Omega_{\pm}/\Omega$  for  $\lambda = 0.05$  where it becomes evident that the light and the matter excitations hybridize and an avoided crossing takes place at the resonance point  $\gamma_2 = 1$ . This signifies the strong coupling between light and matter. Before and after  $\gamma_2 = 1$  the polaritonic excitations lie on top of the bare system excitations, i.e.  $\omega$  and  $\Omega$  respectively. Increasing the light-matter coupling by an order of magnitude to  $\lambda = 0.5$  as shown in Fig. 3(b), leads to a considerably larger Rabi splitting among the branches. The associated polariton gap is comparable to the bare excitations of the system. This is a manifestation of the ultrastrong coupling regime [21], where the polaritons deviate for a larger range of  $\gamma_2$  from the bare excitations as compared to smaller values of  $\gamma_2$ . Turning to the case at which  $\lambda = 1$  [Fig. 3(c)], i.e. bringing the system to the deep strong coupling regime as defined in Ref [21], it becomes apparent that the Rabi split is arguably more pronounced. Also, the upper polariton deviates almost entirely from the the bare excitations of the system and it actually does not reach the bare photon excitation for  $\gamma_2 > 1$  but goes parallel to it. This phenomenon where the polaritons do not reach the bare excitations when depart from the resonance point has also been reported experimentally in Landau polariton systems [42]. Overall, Figs. 2 and 3 convey that the Rabi splitting can be controlled by the number of particles  $N$ , which enters the definition of the interaction parameter  $\lambda$  [Eq. (24)], as a consequence of the collective coupling of the particles to the cavity mode through the CM. Such a collective (or cooperative) behavior has been observed experimentally for magnonic solid-state systems coupled to a photon mode and it was dubbed as “Dicke cooperativity” [87].

## 4 Cavity Induced Localization and Resonance Effect

After describing the photonic properties of the polariton ground state, we focus on the impact of the light field on the matter subsystem, by examining cavity-modified localization properties of matter and its effective mass. To this end, we first inspect the impact of the light-matter coupling on

the ground state density profile of the CM. Utilizing, the polariton coordinates  $S_{\nu+} = (V_{\nu+} - \Lambda V_{\nu-})/\sqrt{1 + \Lambda^2}$  and  $S_{\nu-} = (V_{\nu-} + \Lambda V_{\nu+})/\sqrt{1 + \Lambda^2}$ , the form of  $V_{\nu+} = K_{\nu} \sqrt{\hbar^2/m\Omega^2}$  as well as  $V_{\nu-} = -u_{\nu} \sqrt{\hbar/\tilde{\omega}}$ , the ground state wavefunction reads

$$\Psi_{\text{gs}} = \prod_{\nu=x,y} \phi_0(S_{\nu+}) \otimes \phi_0(S_{\nu-}) = \prod_{\nu=x,y} e^{-\frac{\Omega_+ (K_{\nu} \sqrt{\hbar^2/m\Omega^2} + \Lambda u_{\nu} \sqrt{\hbar/\tilde{\omega}})^2}{2\hbar(1+\Lambda^2)}} e^{-\frac{\Omega_- (\Lambda K_{\nu} \sqrt{\hbar^2/m\Omega^2} - u_{\nu} \sqrt{\hbar/\tilde{\omega}})^2}{2\hbar(1+\Lambda^2)}}, \quad (25)$$

where, for simplicity, we have omitted the normalization constant. For the density profile we express the wavefunction in real space through a Fourier transform, and integrate out the photonic coordinates  $u_{\nu}$ . This leads to the CM density profile

$$n_{\text{cm}}(\mathbf{R}) = \frac{|\Psi_{\text{gs}}(\mathbf{R})|^2}{|\Psi_{\text{gs}}(0)|^2} = \exp\left(-\frac{m_{\text{eff}}\Omega\mathbf{R}^2}{\hbar}\right), \quad (26)$$

with the effective mass

$$m_{\text{eff}} = m \frac{1 + \Lambda^2}{\Omega_+/\Omega + \Lambda^2\Omega_-/\Omega}. \quad (27)$$

It is clear that the density profile of the CM,  $n_{\text{cm}}(\mathbf{R})$ , has a Gaussian form. Importantly, the shape of this Gaussian is modified by the effective mass parameter  $m_{\text{eff}}$  which depends on the polariton modes  $\Omega_+$ ,  $\Omega_-$  and the mixing parameter  $\Lambda$ . This means that the polariton formation modifies the localization properties of the many-body system. To understand the effect of the light-matter coupling on the localization properties of the matter, we present in Fig. 4 the one-dimensional density profile of the CM wavefunction  $n_{\text{cm}}(X)$  for different values of the light-matter coupling. We note that since the effective mass is the same in both directions it is sufficient to focus on the density profile only in the  $X$  coordinate and integrate over the  $Y$  coordinate. As it can be directly seen from Fig. 4 the density profile gradually “shrinks” for increasing  $\lambda$ . This effect stems from the coupling to the light field and it is therefore a cavity-induced localization phenomenon on the many-body system. A similar phenomenon has also been recently reported for an ensemble of two-level systems in waveguide QED [88].

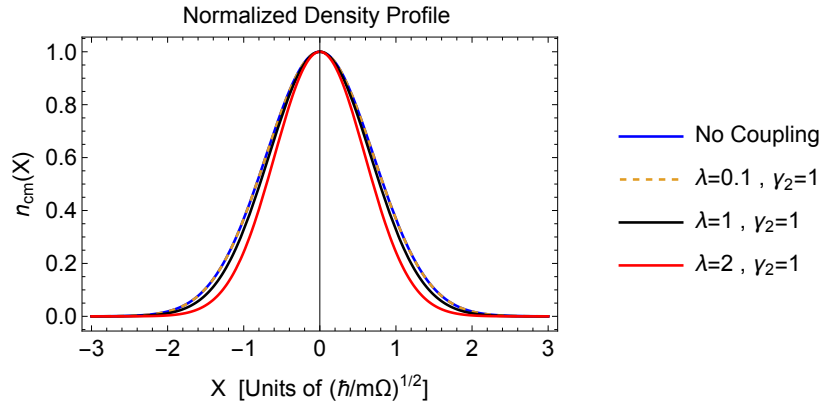


Figure 4: Normalized integrated density profile of the CM wavefunction  $n_{\text{cm}}(X)$  for different values of the light-matter coupling constant  $\lambda$  (see legend) and  $\gamma_2 = 1$ . Evidently, for larger  $\lambda$  the CM density profile experiences a gradually increasing localization behavior which is induced by the cavity.

To further appreciate the cavity-induced localization as captured by the density profile, we explore the behavior of its full-width-at-half-maximum (FWHM). The latter is proportional to the standard deviation  $\sigma$ , namely  $\text{FWHM} = 2\sqrt{2\ln 2}\sigma$ , and quantifies the spatial localization of the density. In particular, for the Gaussian density  $n_{\text{cm}}(X)$  under the influence of the cavity field,  $\sigma = \sqrt{\hbar/2m_{\text{eff}}\Omega}$ , while in the case of no cavity field it is  $\sigma_0 = \sqrt{\hbar/2m\Omega}$ . As such the impact of the light-matter coupling can be measured by  $\text{FWHM}/\text{FWHM}_0 = \sigma/\sigma_0 = \sqrt{m/m_{\text{eff}}}$ . This means that density modifications are reflected in the relative effective mass  $m_{\text{eff}}/m$ . In what follows, we examine the response of  $m_{\text{eff}}/m$  for varying light-matter coupling  $\lambda$  and relative cavity frequency  $\gamma_2 = \omega/\Omega$ .

#### 4.1 Effective mass increase and resonance effect

Figure 5 shows  $m_{\text{eff}}/m$  as a function of  $\lambda$  for several values of  $\gamma_2$ . It is observed that independently of  $\gamma_2$  the effective mass increases for larger  $\lambda$ . This behavior is a direct consequence of the light induced dressing to the matter field. Especially, in the region  $0 < \lambda < 2$  the effective mass features a quadratic increase with respect to  $\lambda$ , and beyond this region  $m_{\text{eff}}$  grows in a linear fashion.

The rate of increase of  $m_{\text{eff}}$  is determined by  $\gamma_2$ . Interestingly, at resonance  $\gamma_2 = 1$  the effective mass experiences a relatively faster increase as compared to other values of  $\gamma_2$  and also its magnitude is maximized. This implies that when the cavity is at resonance with the trap frequency the dressing of matter by the cavity photons is maximized. In the decoupling limit ( $\lambda \rightarrow 0$ ) it holds that  $m_{\text{eff}} = m$ , as expected due to vanishing dressing. Nevertheless, the impact of finite  $\lambda$  on the polariton effective mass is arguably noticeable especially for  $\lambda > 1$ . This facilitates the experimental detection of  $m_{\text{eff}}$  in contrast, for instance, to a phononic dressing cloud [89, 90].

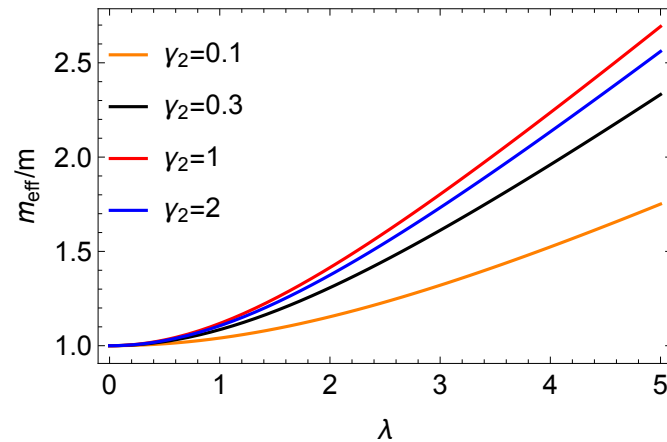


Figure 5: Effective mass ratio  $m_{\text{eff}}/m$  as a function of the light-matter coupling  $\lambda \sim \sqrt{N}$  for fixed  $\gamma_2 = \omega/\Omega$  (see legend). The effective mass becomes larger with increasing  $\lambda$ , while it features its maximal enhancement at resonance, i.e. for  $\gamma_2 = 1$ .

To understand better the aforementioned resonance effect on the effective mass we provide in Fig. 1(b)  $m_{\text{eff}}/m$  in terms of  $\gamma_2 = \omega/\Omega$  for fixed values of  $\lambda$ . We observe that for all  $\lambda$  the effective mass grows rapidly in the region  $0 \leq \gamma_2 \leq 1$ , it reaches a maximum at resonance  $\gamma_2 = 1$  and afterwards decreases approaching asymptotically its bare value,  $m_{\text{eff}} \rightarrow m$ . This essentially

means that when  $\omega \gg \Omega$  the matter subsystem experiences a gradually lesser influence by the cavity field. This resonance phenomenon imprinted as a maximization of the effective mass could potentially provide insights with respect to the resonance effect that is observed in polaritonic chemistry. In this context, alterations of the chemical reactions and properties depend crucially on the resonance between the vibronic excitations and the cavity mode [5–7, 25, 68, 69].

## 5 Cavity Induced Effective Matter Hamiltonian

The fact that the CM density gets modified by the cavity can be also understood in terms of an effective potential that the CM experiences due to the presence of the cavity. This is a common approach in quasi-particle physics [91–93]. Indeed, besides the external trap  $V(\mathbf{R}) = m\Omega^2\mathbf{R}^2/2$ , in the presence of the cavity the CM feels also the effective potential  $V_{\text{eff}}(\mathbf{R}) = m_{\text{eff}}\Omega^2\mathbf{R}^2/2$ . Notice that this scalar potential has precisely the same effect on the CM density profile as the one described by Eq. (26). Thus, the cavity-mediated potential reads  $V_{\text{cav}}(\mathbf{R}) = V_{\text{eff}}(\mathbf{R}) - V(\mathbf{R}) = \delta m\Omega^2\mathbf{R}^2/2$  where  $\delta m = m_{\text{eff}} - m$ . The cavity induced potential introduces a modified harmonic trap for each particle and most importantly it accounts for an extra bilinear or dipole-dipole interaction between the particles. This can be directly seen by expanding  $V_{\text{cav}}$  in terms of the original single-particle coordinates  $\{\mathbf{r}_i\}$

$$V_{\text{cav}}(\mathbf{r}_i, \mathbf{r}_j) = \frac{\delta m\Omega^2}{2N} \left[ \sum_{i=1}^N \mathbf{r}_i^2 + 2 \sum_{i<j}^N \mathbf{r}_i \cdot \mathbf{r}_j \right]. \quad (28)$$

This demonstrates clearly that the cavity field mediates dipole-dipole interactions between the particles and allows us to construct an effective purely matter Hamiltonian for the description of harmonically trapped many-body systems strongly coupled to a cavity.

The corresponding effective Hamiltonian describing *only matter degrees of freedom* reads

$$\hat{H}_{\text{eff}} = \sum_{i=1}^N \left[ -\frac{\hbar^2}{2m} \nabla_i^2 + \left( m + \frac{\delta m}{N} \right) \frac{\Omega^2 \mathbf{r}_i^2}{2} \right] + \sum_{i<l}^N \left[ W(|\mathbf{r}_i - \mathbf{r}_l|) + \frac{\delta m\Omega^2}{N} \mathbf{r}_i \cdot \mathbf{r}_l \right]. \quad (29)$$

It provides an exact description for the ground state properties of the matter subsystem under the influence of a cavity, because it captures the fundamental localization of the CM wavefunction, without the need to account for the photonic states. The inclusion of the latter significantly enlarges the matter-photon Hilbert space and the complexity of the problem. It is important to mention that the derived cavity-induced two-body potential  $V_{\text{cav}}(\mathbf{r}_i, \mathbf{r}_j)$  includes the resonant effect originating from the dependence of  $\delta m$ . However, for the excited states of the matter subsystem the effective Hamiltonian provides only an approximate description, because the cavity potential was derived from the modification of the ground state density. Similar “photon-free” approaches to light-matter interactions have also been put forward recently in the framework of quantum electrodynamical density functional theory (QEDFT) [94].

## 6 Photon Occupations & Photon Correlations

In this section we analyze the photonic properties of the polaritonic ground state, and in particular, the photon occupation in the ground state of the system and the respective photon correlations.

The above will allow us to understand better the nature of the polaritonic ground state shedding also light on the implications of polariton formation.

## 6.1 Photon occupations & two-photon processes

First we calculate the photon occupation in the light-matter ground state. The photon operators can be written as combinations of polariton operators  $\{\hat{d}_{\nu l}, \hat{d}_{\nu l}^\dagger\}$  (see Appendix B for details), namely

$$\hat{a}_\nu = \frac{-1}{\sqrt{4+4\Lambda^2}} \left[ \frac{\omega + \Omega_-}{\sqrt{\Omega_- \omega}} \hat{d}_{\nu-} + \frac{\omega - \Omega_-}{\sqrt{\Omega_- \omega}} \hat{d}_{\nu-}^\dagger - \Lambda \left( \frac{\omega + \Omega_+}{\sqrt{\omega \Omega_+}} \hat{d}_{\nu+} + \frac{\omega - \Omega_+}{\sqrt{\omega \Omega_+}} \hat{d}_{\nu+}^\dagger \right) \right], \quad (30)$$

while  $\hat{a}_\nu^\dagger$  is easily obtained by conjugation. The ground state of the electron-photon system is  $|\Psi_{\text{gs}}\rangle = \prod_\nu |0_+\rangle_\nu |0_-\rangle_\nu$  which is annihilated by both polariton operators  $\hat{d}_{\nu+}$  and  $\hat{d}_{\nu-}$ , i.e.,  $\hat{d}_{\nu\pm} |\Psi_{\text{gs}}\rangle = 0$ . Thus, the photon occupation in the ground state turns out to be

$$\langle \hat{a}_\nu^\dagger \hat{a}_\nu \rangle_{\text{gs}} = \frac{1}{4+4\Lambda^2} \left[ \frac{\Omega_-/\Omega}{\gamma_2} + \frac{\gamma_2}{\Omega_-/\Omega} - 2 + \Lambda^2 \left( \frac{\Omega_+/\Omega}{\gamma_2} + \frac{\gamma_2}{\Omega_+/\Omega} - 2 \right) \right], \quad (31)$$

where the relative polariton modes  $\Omega_-/\Omega$ ,  $\Omega_+/\Omega$  and the relative cavity frequency  $\gamma_2$  have been introduced. The above result is important as it demonstrates that due to the light-matter interaction there are virtual photons occupying the polaritonic ground state. The amount of photons in the ground state depends crucially on the ratio between the polariton modes  $\Omega_\pm$  and the bare cavity frequency  $\omega$ . The behavior of the photon occupation in the ground state is shown in Fig. 6(a) as a function of  $\lambda$  for different  $\gamma_2 = \omega/\Omega$ . We observe that in the interval  $0 \leq \lambda \leq 2$ , the photon occupation increases approximately quadratically in terms of  $\lambda$  independently of  $\gamma_2$ . This fact can be understood from the fit that we perform on the curve characterizing the photon population with  $\gamma_2 = 0.1$  in Fig. 6(a). Since the light-matter coupling is proportional to  $\sqrt{N}$ , the photon occupation is proportional to  $\langle \hat{a}_\nu^\dagger \hat{a}_\nu \rangle_{\text{gs}} \sim N$ , in the region  $0 \leq \lambda \leq 2$ . Despite this, the photon occupation does not overcome unity, because the proportionality constant in the definition of  $\lambda$  [see Eq. (24)] is a small number and the photon occupation per particle is miniscule. This means that there is no macroscopic photon occupation (or superradiant ground state phase), as predicted for the Dicke model [70]. This is a consequence of keeping in the Pauli-Fierz Hamiltonian [Eq. (1)], the diamagnetic  $\mathbf{A}^2$  term. The importance of the diamagnetic term and its connection to the superradiant phase transition will be discussed in more detail in Sec. 7.

For  $\lambda > 2$ , the photon occupation deviates from the quadratic behavior exhibiting a linear trend [Fig. 6(a)]. This implies that in the thermodynamic limit the  $\langle \hat{a}_\nu^\dagger \hat{a}_\nu \rangle_{\text{gs}} \sim \sqrt{N}$  and consequently the photon occupation per particle,  $\langle \hat{a}_\nu^\dagger \hat{a}_\nu \rangle_{\text{gs}}/N$ , vanishes. This behavior has also been identified in the (many-body) Sommerfeld model coupled to the cavity reported, for instance, in Ref. [64]. Another interesting feature is that for smaller values of  $\gamma_2 = \omega/\Omega$  the photon occupation is larger because one matter excitation  $\Omega$  results into several photonic excitations  $\omega$ , i.e., to create a photon costs less energy when  $\omega$  is small. Finally, notice that for  $\lambda \rightarrow 0$  the photon occupation is zero as expected in the decoupling limit.

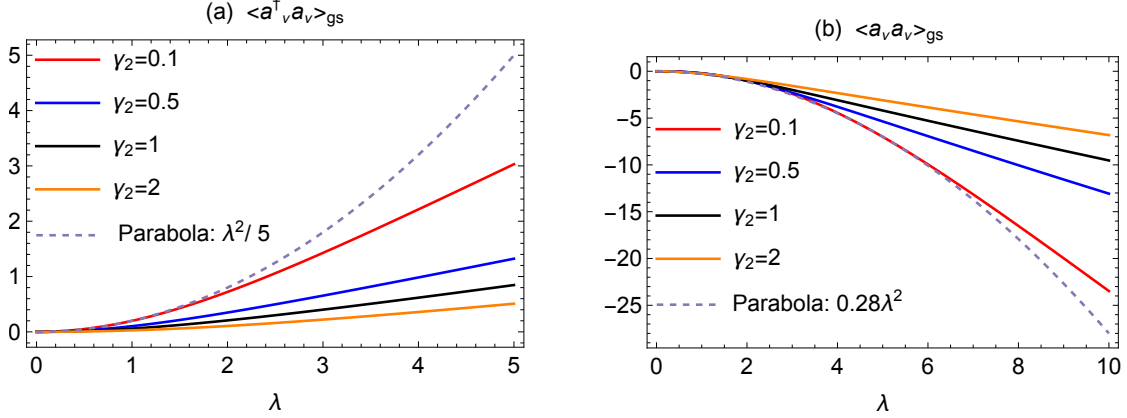


Figure 6: (a) Ground state photon occupation  $\langle \hat{a}_v^\dagger \hat{a}_v \rangle_{\text{gs}}$  and (b) two-point photon function  $\langle \hat{a}_v \hat{a}_v \rangle_{\text{gs}}$  with respect to the light-matter coupling  $\lambda \sim \sqrt{N}$  for several values of the relative cavity frequency  $\gamma_2 = \omega/\Omega$ . The photon occupation increases for larger  $\lambda$ , while the enhanced magnitude of the two-point function indicates the amplified participation of two photon processes. In both panels a quadratic fit (dashed line) corresponding to the curves with  $\gamma_2 = 0.1$  is provided.

Moreover, it is interesting to examine the two-point photon function  $\langle \hat{a}_v \hat{a}_v \rangle_{\text{gs}} = \langle \hat{a}_v^\dagger \hat{a}_v^\dagger \rangle_{\text{gs}}$ . It conveys information on virtual two-photon excitations/de-excitations in the polaritonic ground state. Upon using Eq. (30), introducing the relative cavity frequency  $\gamma_2 = \omega/\Omega$  and the relative polariton frequencies  $\Omega_{\pm}/\Omega$ , it is possible to obtain the two-point function

$$\langle \hat{a}_v \hat{a}_v \rangle_{\text{gs}} = \frac{1}{4 + 4\Lambda^2} \left[ \frac{\gamma_2}{\Omega_-/\Omega} - \frac{\Omega_-/\Omega}{\gamma_2} + \Lambda^2 \left( \frac{\gamma_2}{\Omega_+/\Omega} - \frac{\Omega_+/\Omega}{\gamma_2} \right) \right]. \quad (32)$$

The two-point function is illustrated in Fig. 6(b) with respect to  $\lambda$  and for different values of  $\gamma_2$ . It increases in magnitude for larger  $\lambda$  meaning that more two-photon processes occur in the polariton ground state for stronger light-matter coupling. As in the case of the photon occupation [Fig. 6(a)] the trend of  $\langle \hat{a}_v \hat{a}_v \rangle_{\text{gs}}$  is initially ( $\lambda < 2$ ) quadratic (see also the fitted quadratic curve in Fig. 6(b) for  $\gamma_2 = 0.1$ ) and then becomes linear. Notably, however, the rate of increase of the two-point function is larger than the one of the photon occupation and most importantly it features a quadratic trend for a much more extensive  $\lambda$  interval. For example, for  $\gamma_2 = 0.1$  the two-point function behaves quadratically in the region  $0 \leq \lambda \leq 6$ . These two differences on the behavior of  $\langle \hat{a}_v^\dagger \hat{a}_v \rangle_{\text{gs}}$  and  $\langle \hat{a}_v \hat{a}_v \rangle_{\text{gs}}$  will be proved crucial for the discussion of the photon statistics in the next subsection. It is important to highlight that the photon occupation  $\langle \hat{a}_v^\dagger \hat{a}_v \rangle_{\text{gs}}$  or the two-point function  $\langle \hat{a}_v \hat{a}_v \rangle_{\text{gs}}$  *on their own* do not provide information about the character, statistics or correlations of the photons. The quantity that gives insights into the photon correlations and statistics is the Mandel  $Q$  parameter [65] which we analyze below.

## 6.2 Photon correlations

The Mandel  $Q$  parameter measures the deviation of the photon statistics from the Poisson distribution [65]. It is defined as

$$Q_v = \frac{\langle \hat{a}_v^\dagger \hat{a}_v^\dagger \hat{a}_v \hat{a}_v \rangle - \langle \hat{a}_v^\dagger \hat{a}_v \rangle^2}{\langle \hat{a}_v^\dagger \hat{a}_v \rangle}. \quad (33)$$



If it takes values in the range  $-1 \leq Q < 0$ , then the photons follow sub-Poissonian statistics and experience an antibunching behavior, which is a feature of non-classical light. However, thermal photons are characterized by  $Q > 0$  and obey super-Poissonian statistics (bunching). For  $Q = 0$ , photons are represented by a coherent state and obey Poisson statistics [65, 67, 95].

It can be proved that the  $Q$  parameter for the polaritonic ground state  $|\Psi_{\text{gs}}\rangle = \prod_{\nu} |0_{+}\rangle_{\nu} |0_{-}\rangle_{\nu}$ , with  $\langle \hat{a}^{\dagger} \hat{a} \rangle_{\text{gs}}$  given in Eq. (31), and the four-point function  $\langle \hat{a}_{\nu}^{\dagger} \hat{a}_{\nu}^{\dagger} \hat{a}_{\nu} \hat{a}_{\nu} \rangle_{\text{gs}} = 2\langle \hat{a}_{\nu}^{\dagger} \hat{a}_{\nu} \rangle_{\text{gs}}^2 + \langle \hat{a}_{\nu} \hat{a}_{\nu} \rangle_{\text{gs}}^2$  evaluated using Eq. (33) (see also Appendix C) has the form,

$$Q_{\nu} = \frac{\langle \hat{a}_{\nu}^{\dagger} \hat{a}_{\nu} \rangle_{\text{gs}}^2 + \langle \hat{a}_{\nu} \hat{a}_{\nu} \rangle_{\text{gs}}^2}{\langle \hat{a}_{\nu}^{\dagger} \hat{a}_{\nu} \rangle_{\text{gs}}}. \quad (34)$$

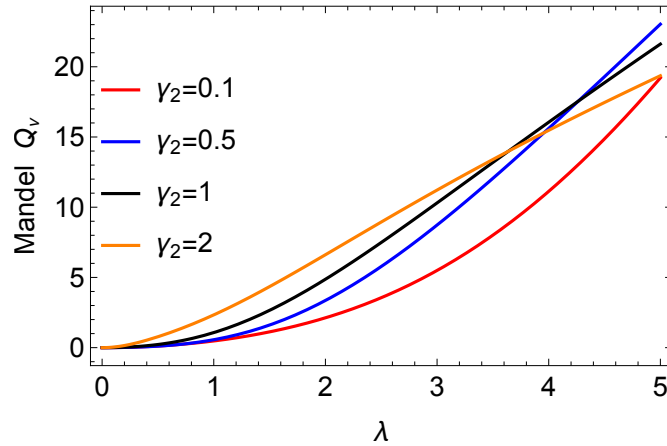


Figure 7: Mandel  $Q$  parameter identifying photon-photon correlations in terms of  $\lambda$  and fixed values of  $\gamma_2 = \omega/\Omega$ .  $Q$  is positive meaning that the photons in the polariton ground state satisfy super-Poissonian statistics and are of thermal character, a behavior that becomes enhanced for larger  $\lambda$ . Crossings of  $Q$  corresponding to different  $\gamma_2$  at specific  $\lambda$  reveal the interplay between photon occupation and the two-point function depicted in Fig. 6.

From the previous expression it is clear that the Mandel  $Q$  parameter in the polaritonic vacuum is strictly positive because all quantities entering Eq. (34) are positive. The Mandel parameter is proportional to the sum of the quadratures of the photon occupation and the two-point function. Both contributions for non-zero light-matter coupling  $\lambda$  are finite (see Fig. 6) and thus  $Q$  is larger than zero. This implies that the ground state photons satisfy super-Poissonian statistics and thus correspond to thermal (bunched) photons [65, 67]. Accordingly, the light-matter interaction induces non-trivial statistics and correlations between the photons which increase for larger  $\lambda$ , as it can be seen in Fig. 7. Strikingly, the  $Q$  parameter unlike the photon occupations and two-point function, where smaller  $\gamma_2$  results in larger values for all  $\lambda$ , exhibits a more intricate behavior. Particularly, for different values of  $\gamma_2$  crossings appear between the different “trajectories” of the  $Q$  parameter in terms of  $\lambda$  where before the crossing, for example  $Q$  for  $\gamma_2 = 2$  is larger than  $Q$  for  $\gamma_2 = 1$ , while after the crossing the opposite holds. This phenomenon is a consequence of the competition between the photon occupation  $\langle \hat{a}_{\nu}^{\dagger} \hat{a}_{\nu} \rangle_{\text{gs}}$  and the two-point function  $\langle \hat{a}_{\nu} \hat{a}_{\nu} \rangle_{\text{gs}}$ , which

as we described previously, behave differently as a function of  $\lambda$ . This demonstrates that with strong and ultrastrong light-matter coupling it is possible to tailor the photon statistics and their correlations in a non-trivial fashion. Note that for  $\lambda \rightarrow 0$  it holds  $Q \rightarrow 0$ , which means that in the decoupling limit photons follow trivial Poisson statistics, as expected [65, 67]. It is important to mention that the positivity of the  $Q$  parameter in our system holds in the polariton ground state. However, under external driving, the excited states of the polaritons can be accessed in which the Mandel parameter can become negative. This would signify the generation of non-classical light [67, 96].

## 7 Superradiant Instability

In what follows we are interested in the importance of the often neglected [97] diamagnetic  $\hat{A}^2$  term for our many-body system coupled to the cavity. The influence of this quadratic term on light-matter related phenomena has been studied theoretically in several publications see e.g. Refs. [64, 97–100] and its impact has also been experimentally measured in Landau polariton systems [44]. Importantly, it has been argued that eliminating the  $\hat{A}^2$  term leads to the well-known superradiant phase transition of the Dicke model [83]. This refers to the situation where the ground state of an ensemble of two-level systems coupled to a single quantized mode of the photon field, in the thermodynamic limit, acquires a macroscopic (infinite) photon occupation [70]. The existence though of the superradiant phase was questioned by a no-go theorem where it was shown that once the diamagnetic term is included the superradiant phase transition does not take place [101]. More recently, the possibility of a superradiant phase transition has been suggested [71, 102, 103] but again respective no-go theorems [104–106] have been derived. Lastly, the occurrence of a superradiant phase transition beyond the dipole approximation has also been suggested [107, 108].

In our case, the CM Hamiltonian of the many-body system coupled to the cavity in the absence of the diamagnetic term  $\hat{H}'_{\text{cm}} = \hat{H}_{\text{cm}} - \frac{Ng_0^2}{2m} \hat{A}^2$  is

$$\hat{H}'_{\text{cm}} = -\frac{\hbar^2}{2m} \nabla_{\mathbf{R}}^2 + \frac{ig_0\hbar}{m} \sqrt{N} \hat{\mathbf{A}} \cdot \nabla_{\mathbf{R}} + \frac{m\Omega^2}{2} \mathbf{R}^2 + \sum_{v=x,y} \hbar\omega \left( \hat{a}_v^\dagger \hat{a}_v + \frac{1}{2} \right). \quad (35)$$

The latter can be diagonalized analytically following the procedure described in Sec. 3 with the only difference being that in the absence of the  $\hat{A}^2$  term the bare cavity frequency  $\omega$  *does not get renormalized* by the diamagnetic frequency  $\omega_d$ . Thus, we can straightforwardly obtain the respective polariton modes, see also Eq. (17), which are found to be

$$\Omega'_\pm = \sqrt{\frac{1}{2} \left( \omega^2 + \Omega^2 \pm \sqrt{4\omega_d^2\Omega^2 + (\omega^2 - \Omega^2)^2} \right)}. \quad (36)$$

Without the  $\hat{A}^2$  contribution the lower polariton develops an instability for large values of the light-matter interaction. To demonstrate this, let us consider the resonance scenario  $\omega = \Omega$ . In this case, the lower polariton mode simplifies to  $\Omega'_- = \sqrt{\Omega(\Omega - \omega_d)}$  which implies that for  $\omega_d = \Omega$  ( $\gamma_1 = 1$ ) the lower polariton becomes zero (or gapless) and for  $\omega_d > \Omega$  it becomes imaginary signifying that the light-matter system is unstable. This instability is related to the superradiant phase transition [70]. The connection to the superradiant phase and the macroscopic photon

occupation can be directly understood from the ground state photon occupation  $\langle \hat{a}_\nu^\dagger \hat{a}_\nu \rangle_{\text{gs}}$  given by Eq. (31). Indeed, at the point of the instability where  $\Omega'_- \rightarrow 0$ , the photon occupation diverges

$$\langle \hat{a}_\nu^\dagger \hat{a}_\nu \rangle_{\text{gs}} \rightarrow \infty. \quad (37)$$

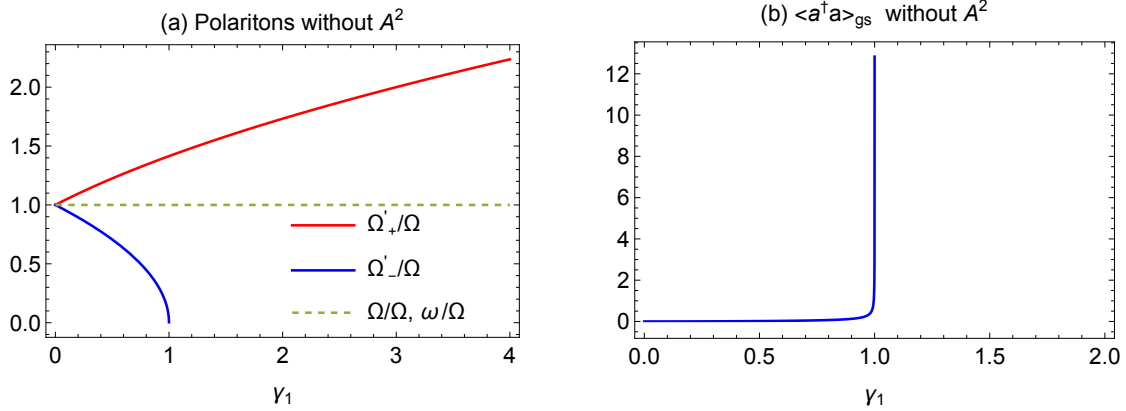


Figure 8: (a) Normalized polariton branches  $\Omega'_\pm/\Omega$  and (b) photon occupation in the absence of the diamagnetic  $A^2$  term as a function of  $\gamma_1 = \omega_d/\Omega$ . As it can be seen, the lower polariton develops an instability as it becomes zero at  $\gamma_1 = 1$ . Accordingly, the photon occupation diverges at the instability point manifesting its superradiant character. The dashed line in (a) corresponds to matter and light excitations which coincide.

This means that there is a macroscopic photon occupation in the ground state, i.e., a photon condensate [70, 106]. These two important consequences of neglecting the diamagnetic term are visualized in Fig. 8. Taking into account the diamagnetic term the system becomes again stable and the photon occupation is finite as it was found in Sec. 6. The fact that the system becomes unstable without the  $\hat{A}^2$  term shows clearly the importance of the diamagnetic interaction which has been largely assumed that it can be neglected or eliminated from the QED Hamiltonian [14, 97]. Similar conclusions were also reached for the Sommerfeld model (free electron gas) coupled to the photon field [64], where it was also argued that as long as the diamagnetic  $\hat{A}^2$  term is kept in the minimal coupling Hamiltonian, the system is stable and no superradiant instability occurs [64].

Our work generalizes this previous result to the case where the two-body interaction between the particles is included and the particles are bound to a scalar harmonic potential. This no-go demonstration is important because it is exact and non-perturbative and does not rely on an asymptotic decoupling between light and matter in the thermodynamic limit [106] or on perturbation theory [107, 108].

## 8 Polariton-Control with a Weak Magnetic Field

Up to here we have examined the polariton properties of the many-body system coupled to the cavity field in the absence of any external perturbation. A natural question that arises concerns the influence of an external weak homogeneous magnetic field on the polariton modes. The Hamiltonian  $\hat{H}_B$  describing the system in the presence of the external magnetic field can be written

as

$$\hat{H}_B = \hat{H} + \sum_{i=1}^N \frac{g_0}{m} (i\hbar\nabla_i + g_0\hat{\mathbf{A}}) \cdot \mathbf{A}_{\text{ext}}(\mathbf{r}_i) + \frac{g_0^2}{2m} \mathbf{A}_{\text{ext}}^2(\mathbf{r}_i), \quad (38)$$

where  $\hat{H}$  denotes the Hamiltonian without the magnetic field [Eq. (1)] for the single-mode case. The other terms account for the vector potential of the magnetic field and appear by considering the vector potential  $\mathbf{A}_{\text{ext}}(\mathbf{r}) = -\mathbf{e}_x B y$ , inducing a homogeneous magnetic field in the  $z$  direction, into the minimal-coupling Hamiltonian [Eq. (1)]. Recall also that the polaritons in the original Hamiltonian  $\hat{H}$  form in the CM frame. For that purpose we transform the total Hamiltonian in the CM and relative coordinates frames. Then, the Hamiltonian reads

$$\hat{H}_B = \hat{H}_{\text{cm}} + \frac{g_0}{m} (i\hbar\nabla_{\mathbf{R}} + g_0\sqrt{N}\hat{\mathbf{A}}) \cdot \mathbf{A}_{\text{ext}}(\mathbf{R}) + \frac{g_0^2}{2m} \mathbf{A}_{\text{ext}}^2(\mathbf{R}) + \hat{H}_{\text{rel}}(\{\mathbf{R}_j, \mathbf{A}_{\text{ext}}(\mathbf{R}_j)\}). \quad (39)$$

For the polariton states the relative degrees of freedom,  $\mathbf{R}_j$  with  $j > 1$ , are irrelevant because they are decoupled from the CM part. Thus, we can neglect  $\hat{H}_{\text{rel}}$ . To find the effect of the magnetic field on the polariton states we express the  $x$ -component of the momentum operator  $\nabla_{\mathbf{R}}$ , the quantized photon field  $\hat{\mathbf{A}}$  and the magnetic field  $\mathbf{A}_{\text{ext}}$  in terms of the polaritonic operators  $\{\hat{d}_{x+}, \hat{d}_{y+}, \hat{d}_{x-}, \hat{d}_{y-}\}$

$$\begin{aligned} i\hbar\nabla_x &= -\sqrt{\frac{\hbar m \Omega}{2 + 2\Lambda^2}} \left[ \Lambda \frac{\Omega}{\sqrt{\Omega\Omega_-}} (\hat{d}_{x-} + \hat{d}_{x-}^\dagger) + \frac{\Omega}{\sqrt{\Omega\Omega_+}} (\hat{d}_{x+} + \hat{d}_{x+}^\dagger) \right], \\ \hat{\mathbf{A}} &= \sqrt{\frac{\hbar}{2\epsilon_0 V \omega}} \frac{-1}{\sqrt{1 + \Lambda^2}} \sum_{\nu=x,y} \mathbf{e}_\nu \left[ \frac{\omega}{\sqrt{\omega\Omega_-}} (\hat{d}_{\nu-} + \hat{d}_{\nu-}^\dagger) + \frac{\omega}{\sqrt{\omega\Omega_+}} (\hat{d}_{\nu+} + \hat{d}_{\nu+}^\dagger) \right], \\ \mathbf{A}_{\text{ext}}(\mathbf{R}) &= \frac{-\mathbf{e}_x iB\sqrt{\hbar}}{\sqrt{2m\Omega(1 + \Lambda^2)}} \left[ \Lambda \sqrt{\frac{\Omega_-}{\Omega}} (\hat{d}_{y-} + \hat{d}_{y-}^\dagger) + \sqrt{\frac{\Omega_+}{\Omega}} (\hat{d}_{y+} + \hat{d}_{y+}^\dagger) \right]. \end{aligned} \quad (40)$$

Here, the relations for the photonic and matter operators in terms of the polaritonic ones provided in Appendix B were used. The strength of the external magnetic field is considered to be weak as compared to the frequency of the trapping potential. This is quantified by the ratio between the magnetic-field dependent frequency  $\omega_B = g_0 B/m$  (analogous to the cyclotron frequency) and the frequency of the trap  $\Omega$ . Thus, the contribution of the magnetic field can be treated perturbatively. To first order in perturbation theory the bilinear term  $(i\hbar\nabla_{\mathbf{R}} + g_0\sqrt{N}\hat{\mathbf{A}}) \cdot \mathbf{A}_{\text{ext}}(\mathbf{R})$  does not contribute to the shift of the polaritonic energy levels. Indeed, this coupling term involves only scatterings between the polaritons in the different directions of the form  $\sim \hat{d}_x \hat{d}_y$  whose expectation value vanishes in the polariton ground state. This implies that only  $\mathbf{A}_{\text{ext}}^2$  modifies the polariton energy levels, which read

$$\delta E_{n_+, n_-} = \frac{g_0^2}{2m} {}_y \langle n_+ | {}_y \langle n_- | \mathbf{A}_{\text{ext}}^2 | n_- \rangle {}_y | n_+ \rangle = \frac{\hbar \omega_B^2}{2\Omega^2} \left[ \frac{\Omega_+}{1 + \Lambda^2} \left( n_+ + \frac{1}{2} \right) + \frac{\Lambda^2 \Omega_-}{1 + \Lambda^2} \left( n_- + \frac{1}{2} \right) \right], \quad (41)$$

with  $\omega_B = g_0 B/m$ . The above result gives the correction to the polariton energy levels (in the  $y$  direction) due to the external magnetic field

$$\delta \Omega_+(B) = \frac{\Omega_+ \omega_B^2}{2\Omega^2(1 + \Lambda^2)} \quad \text{and} \quad \delta \Omega_-(B) = \frac{\Omega_- \omega_B^2 \Lambda^2}{2\Omega^2(1 + \Lambda^2)}. \quad (42)$$

Therefore, the polariton modes under the external perturbation become  $\Omega_+(B) = \Omega_+ + \delta\Omega_+(B)$  and  $\Omega_-(B) = \Omega_- + \delta\Omega_-(B)$ . The polariton branches for varying  $\gamma_2$  are shown in Fig. 9(a). It is evident that within  $\gamma_2 < 1$ , i.e. before the avoided crossing, the energy of the magnetic field is absorbed by the upper polariton while the lower one remains unaffected, see the deviation of each branch from its bare excitation energy. In the vicinity of the avoided crossing,  $\gamma_2 = 1$ , the polariton branches exchange energy and for  $\gamma_2 > 1$  the lower polariton acquires the energy of the upper polariton which turns back to its original unperturbed value. The aforementioned behavior manifests that energy transfer between the two polariton states occurs in the presence of the magnetic field.

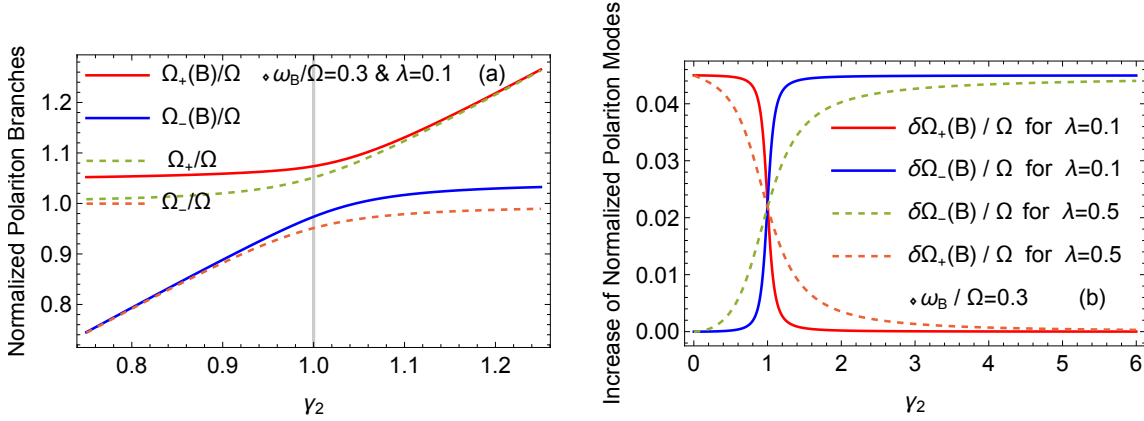


Figure 9: (a) Polariton branches and (b) energy increase of each branch in the presence of an external magnetic field  $B$  with respect to  $\gamma_2 = \omega/\Omega$ . Dashed lines in (a) illustrate the polariton branches in the absence of  $B$ , while in (b) refer to different values of  $\lambda$  (see legend). The magnetic field shifts the point of the avoided crossing (minimum energy difference) and the polariton gap decreases (panel (a)). In (b) the polaritons exchange energy as a function of  $\gamma_2$  and at  $\gamma_2 = 1$  they possess exactly the same energy increase.

To further analyze this energy transfer process we track separately the corrections of the polariton branches  $\delta\Omega_+(B)/\Omega$  and  $\delta\Omega_-(B)/\Omega$ , divided by the trap frequency, as a function of the relative cavity frequency  $\gamma_2$ , see Fig. 9(b). For  $\gamma_2 < 1$  the energy of the magnetic field is absorbed by the upper polariton, while increasing  $\gamma_2$  towards the resonance point ( $\gamma_2 = 1$ ) the upper polariton transfers its energy to the lower one. At the resonance point the two branches  $\delta\Omega_{\pm}(B)/\Omega$  coincide, meaning that the upper polariton has transferred half of its energy to the lower one. As such, the two polaritons acquire exactly the same amount of energy from the magnetic field. Beyond  $\gamma_2 = 1$  the energy of the upper polariton continues to decrease and eventually all the energy is transferred to the lower polariton. At resonance  $\delta\Omega_+(B) = \delta\Omega_-(B)$  independently of the value of the light-matter coupling, as it can be seen from Fig. 9(b), while the rate of the energy exchange depends on  $\lambda$ . These findings pave the way for future investigations devoted to unravel the interplay of interparticle correlations and the energy transfer among the polaritons, especially so by devising specific dynamical protocols.

## 8.1 Behavior of the polariton gap

In addition to the inter-polariton energy exchange there are several other important phenomena that exclusively take place due to the magnetic field. As it can be seen in Fig. 9(a), the polariton

gap closes due to the magnetic field, compare with the gap among the bare excitation energies depicted with the dashed lines. The key observation is that the point at which the polaritons actually come to the closest proximity is no longer the resonance point  $\gamma_2 = 1$ . This can be understood through the energy gap  $\Delta_B = \Omega_+(B) - \Omega_-(B)$  between the polaritons as a function of the magnetic field

$$\frac{\Delta_B}{\Omega} = \frac{\Omega_+ - \Omega_-}{\Omega} + \frac{\omega_B^2}{2\Omega^2(1 + \Lambda^2)} \left( \frac{\Omega_+}{\Omega} - \Lambda^2 \frac{\Omega_-}{\Omega} \right). \quad (43)$$

The first term refers to the gap  $\Delta$  for zero magnetic field and only the second contribution depends on the strength of the magnetic field  $B$  through  $\omega_B$ . Figure 10 presents the behavior of the normalized gap  $\Delta_B/\Omega$  for different values of  $\gamma_2$  and of the magnetic field. Particularly, Fig. 10(a) depicts  $\Delta_B/\Omega$  as a function of  $\gamma_2$  with fixed magnetic field ( $\omega_B/\Omega$ ) and in Fig. 10(b) we fix  $\gamma_2$  showcasing the gap in terms of  $\omega_B/\Omega$ . In both cases the value of the gap at the resonance point  $\gamma_2 = 1$  is not affected by the magnetic field. This is true because at  $\gamma_2 = 1$  the second term in Eq. (43) vanishes. Moreover, we readily observe that beyond the resonance point, i.e., for  $\gamma_2 > 1$ , the polariton gap in the presence of the magnetic field can become smaller as compared to  $\gamma_2 = 1$ . This does not occur for all values of the magnetic field but only after a particular critical value of  $\omega_B/\Omega$  as shown in Fig. 10(b). This non-trivial dependence of the polariton gap to the magnetic field strength is important for the associated Landau-Zener transition probability [72] which we discuss below.

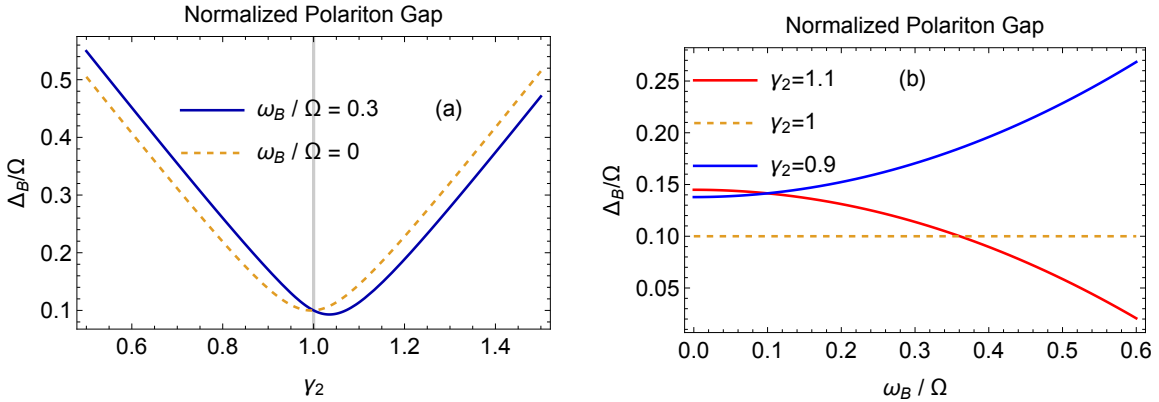


Figure 10: Normalized polariton gap  $\Delta_B/\Omega$  in the presence of a weak external magnetic field. (a)  $\Delta_B/\Omega$  with respect to  $\gamma_2$  and (b) in terms of  $\omega_B/\Omega$ . In both cases the polariton gap at resonance  $\gamma_2 = 1$  is not affected by the magnetic field while beyond the resonance point, and for particular values of the magnetic field, becomes smaller than the gap at resonance.

## 8.2 Landau-Zener transition

The width of the avoided crossing between the polaritons can be manipulated by the external magnetic field. As a consequence, it also influences the probability of a diabatic transition in the vicinity of the avoided crossing between the polariton branches. This probability is given by the well-known Landau-Zener formula [72]  $P_{LZ} = e^{-2\pi\Gamma}$  with  $\Gamma = \frac{\Delta^2}{\hbar|v|}$ . Also,  $\Delta$  is half of the energy difference between the two levels (here the lower polariton branches) at the avoided crossing,  $2\Delta_B = \hbar(\Omega_+(B) - \Omega_-(B))$ , and  $v$  is the Landau-Zener velocity dictating the rate at which the crossing is traversed. We utilize the Landau-Zener formula to infer the probability of a diabatic

transition from the lower to the upper polariton, while varying the cavity frequency by moving slowly the cavity mirrors. To demonstrate the effect of the magnetic field in the underlying transition probability we introduce the relative polariton frequencies  $\Omega_+(B)/\Omega$ ,  $\Omega_-(B)/\Omega$  obtaining  $P_{LZ} = e^{-\frac{\pi\hbar\Omega^2}{2|\nu|} \left(\frac{\Delta_B}{\Omega}\right)^2}$ . The respective Landau-Zener probability as a function of the dimensionless ratio  $\omega_B/\Omega$ , is provided in Fig. 11. It is evident that the Landau-Zener probability at the resonance point  $\gamma_2 = 1$  is independent of  $\omega_B/\Omega$ , and hence  $B$ . This is a consequence of the robustness of the polariton gap against the magnetic field at  $\gamma_2 = 1$  as we discussed previously, see also Fig. 10. Turning to  $\gamma_2 > 1$  [Fig. 11], there is a critical magnetic field strength above which the Landau-Zener probability becomes larger than the one at resonance. This observation implies that an external magnetic field can be used to control the point at which a Landau-Zener transition between the polaritons takes place. In this sense, there is an interesting interplay between the polariton states due to the external magnetic field, which can be utilized to tune some of their fundamental properties, as well as generate an exchange of energy between them.

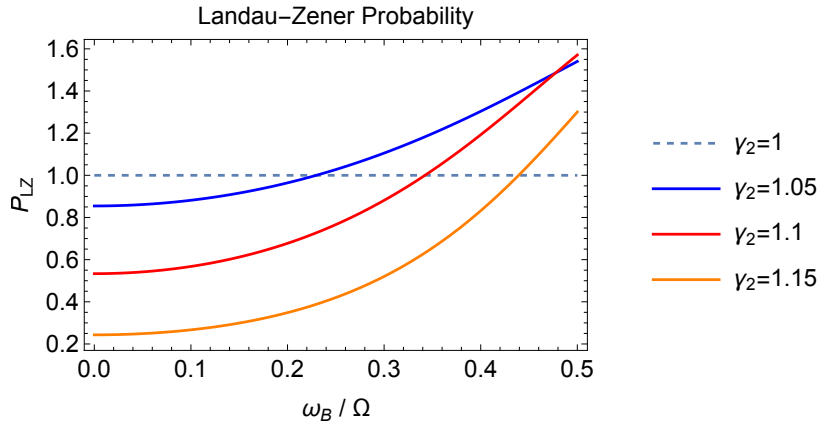


Figure 11: Landau-Zener probability as a function of the magnetic field dependent parameter  $\omega_B/\Omega = g_0 B/m\Omega$  for different values of  $\gamma_2$  and for  $\hbar\Omega^2/2|\nu| = 2$ . It becomes clear that for  $\gamma_2 > 1$ , i.e. beyond the resonance point, there is a critical value of the magnetic field at which the transition probability becomes larger than the one at resonance  $\gamma_2 = 1$ .

## 9 Summary and Outlook

We study the formation of collective polariton states emerging in a harmonically trapped many-body interacting system, strongly coupled to a spatially homogeneous cavity field. We demonstrate that the light field couples to the particle CM, while creating an effective dipolar potential in the relative coordinates in which particle-particle interactions emerge. As such, it was possible to analytically obtain the exact many-body polariton states and describe various light-induced phenomena including the increase of the effective mass of the particles, effective interactions mediated in the matter subsystem by the cavity field and the behavior of photon correlations.

By inspecting the matter subsystem we exemplify that the cavity field enhances the spatial localization of the many-body system. The cavity-induced localization manifests itself as a shrinking of the CM density profile which becomes more prominent in the ultrastrong coupling regime. The localization phenomenon is related to the increase of the effective mass of the particles [64]

---

and can be understood in terms of cavity mediated interactions between the particles in the polaritonic ground state. A corresponding effective potential picture mediated by the cavity field into the matter subsystem is also derived, yielding an enhanced external trap for the matter field but most importantly induced dipole-dipole interactions. Another interesting feature imprinted in the behavior of the effective mass (and the cavity induced potential) is that it exhibits a maximum at the point of resonance between the cavity and the matter excitation. This resonance effect could potentially provide insights on the resonance effect observed in polaritonic chemistry [5–7, 25, 68, 69].

The polaritonic ground state, being a correlated state between photons and matter, contains a non-trivial photon population [64]. Particularly, due to the matter-mediated correlations, the photons obey super-Poissonian statistics implying that we have bunched or otherwise thermal photons [67, 95, 109].

Turning to the impact of the often neglected diamagnetic interactions we showcase that if the  $A^2$  term is dropped the system develops an instability. The latter manifests by the fact that the lower polariton at a critical value of the light-matter interaction goes to zero, and beyond this critical point becomes imaginary signifying that the Hamiltonian becomes unstable. This is a behavior similar to the one discussed in Ref. [71] for the Hopfield model [110]. At the critical point the ground-state photon occupation diverges, which means that photon condensation occurs [106, 108], and thus the instability is of superradiant character [70]. However, as long as the diamagnetic term is taken into account, the composite system is stable independently of the light-matter coupling and the photon occupation is finite implying that the superradiant phase transition is prevented.

Upon considering an external perturbation, through a homogeneous magnetic field, we reveal that it substantially affects the properties of the polariton branches. Indeed, it induces a coherent energy transfer among the polaritons which acquire exactly the same amount of energy at resonance. Accordingly, the polariton gap at resonance is insensitive to magnetic field variations. Otherwise, the polariton gap is affected differently below and above resonance. Namely, below (above) resonance the gap is larger (smaller) than at resonance. This phenomenon has direct implications on the respective Landau-Zener transition probability [72] between the polaritons. Due to the gap closing beyond the resonance point, the underlying transition probability is enhanced via the magnetic field.

Our work provides analytical insights to strong and ultrastrong light-matter interactions and paves the way for several future directions aiming to reveal polariton phenomena in many-body cavity QED settings. An interesting possibility is to generalize our treatment, introduced in Sec. 2.1, in order to study many-body polariton states, in multi-mode cavities which are currently of intense theoretical and experimental interest [111, 112]. Employing a homogeneous time-dependent electric field it would be possible to probe the dynamical formation of polariton states and in general monitor their non-equilibrium time-evolution. Certainly, a deeper understanding of the cavity mediated interactions between the particles (discussed in Sec. 5) and the range of validity of the effective Hamiltonian approach (Eq. (28)) are worth to be pursued. This will allow us to describe the impact of the cavity field on the ground-state of the many-body system, without the need to explicitly treat the photonic states. For the excited states, the effective Hamiltonian provides only an approximate description. Similar “photon-free” approaches to light-matter interactions have also been put forward recently in the framework of QEDFT [94], and potentially the cavity potential that we constructed could be useful for the QEDFT framework as well. Additionally, the consideration of a two-component system inside the cavity will give rise to several interesting phenomena. For instance, it is expected that the presence of two-body inter-component coupling



will facilitate the generation of mediated interactions between the polariton quasiparticles of the different components [24]. These polariton-polariton interactions [113, 114] will introduce polariton non-linearities [115] which could potentially lead to polariton condensation [116]. Finally, polariton-polariton interactions can also emerge, even for a single component system, e.g. by considering an inhomogeneous cavity field.

## Acknowledgements

We would like to thank Dan Stamper-Kurn for fruitful discussions. The authors acknowledge support from the NSF through a grant for ITAMP at Harvard University. S. I. M. was also supported in part by the National Science Foundation under Grant No. NSF PHY-1748958.

## A Exact Solution in Free Space

In this Appendix we focus on the case where the matter subsystem lies in free space without an external trap, i.e.,  $\Omega = 0$ . As we already explained within the main text in Sec. 2, the relative coordinate part of the Hamiltonian does not couple to the quantized light field. Thus, from the perspective of the light-matter interaction the relative part is not relevant. As a consequence we only focus on the CM part of the Hamiltonian which in the single-mode case considered throughout [see Eq. (11)] reads

$$\hat{H}_{\text{cm}} = -\frac{\hbar^2}{2m} \nabla_{\mathbf{R}}^2 + ig_0 \hbar \sqrt{N} \hat{\mathbf{A}} \cdot \nabla_{\mathbf{R}} + \underbrace{\frac{Ng_0^2}{2m} \hat{\mathbf{A}}^2 + \sum_{\nu=x,y}^2 \hbar \omega \left[ \hat{a}_{\nu}^{\dagger} \hat{a}_{\nu} + \frac{1}{2} \right]}_{\hat{H}_p}. \quad (44)$$

In the above expression  $\hat{H}_p$  solely depends on the photon annihilation and creation operators i.e.  $\{\hat{a}_{\nu}, \hat{a}_{\nu}^{\dagger}\}$ . As argued in Sec. 3 this Hamiltonian can be brought into a diagonal form by defining the bosonic operators  $\hat{b}_{\nu} = \frac{1}{2\sqrt{\omega\tilde{\omega}}} [\hat{a}_{\nu}(\tilde{\omega} + \omega) + \hat{a}_{\nu}^{\dagger}(\tilde{\omega} - \omega)]$  (and its conjugate  $\hat{b}_{\nu}^{\dagger}$ ). Note, that this transformation is equivalent to the scaling transformation we performed in Sec. 3 on the photonic displacement coordinates. Accordingly, the Hamiltonian takes the form

$$\hat{H}_{\text{cm}} = -\frac{\hbar^2}{2m} \nabla_{\mathbf{R}}^2 + ig \sum_{\nu=x,y} \mathbf{e}_{\nu} (\hat{b}_{\nu}^{\dagger} + \hat{b}_{\nu}) \cdot \nabla_{\mathbf{R}} + \sum_{\nu=x,y}^2 \hbar \tilde{\omega} \left( \hat{b}_{\nu}^{\dagger} \hat{b}_{\nu} + \frac{1}{2} \right). \quad (45)$$

Recall that  $g = \omega_d \sqrt{\hbar^3/2m\tilde{\omega}}$  is the collective light-matter coupling constant. The Hamiltonian of Eq. (45) is invariant under translations in the matter configuration space, since it only includes the momentum operator of the particles. This implies that  $\hat{H}_{\text{cm}}$  commutes with the momentum operator  $\nabla$ ,  $[\hat{H}_{\text{cm}}, \nabla_{\mathbf{R}}] = 0$ , and the eigenfunctions of the CM are plane waves of the form  $\phi_{\mathbf{K}} = e^{i\mathbf{K}\cdot\mathbf{R}}/\sqrt{V}$ . Applying the Hamiltonian  $\hat{H}_{\text{cm}}$  on the eigenfunction  $\phi_{\mathbf{K}}$  we have

$$\hat{H}_{\text{cm}} \phi_{\mathbf{K}} = \left[ \sum_{\nu=x,y}^2 \left[ \hbar \tilde{\omega} \left( \hat{b}_{\nu}^{\dagger} \hat{b}_{\nu} + \frac{1}{2} \right) - g (\hat{b}_{\nu} + \hat{b}_{\nu}^{\dagger}) \mathbf{e}_{\nu} \cdot \mathbf{K} \right] + \frac{\hbar^2 \mathbf{K}^2}{2m} \right] \phi_{\mathbf{K}}. \quad (46)$$

Defining now another set of annihilation and creation operators  $\{\hat{c}_{\nu}^{\dagger}, \hat{c}_{\nu}\}$

$$\hat{c}_{\nu} = \hat{b}_{\nu} - \frac{g \mathbf{e}_{\nu} \cdot \mathbf{K}}{\hbar \tilde{\omega}} \quad \text{and} \quad \hat{c}_{\nu}^{\dagger} = \hat{b}_{\nu}^{\dagger} - \frac{g \mathbf{e}_{\nu} \cdot \mathbf{K}}{\hbar \tilde{\omega}}, \quad (47)$$

the operator  $\hat{H}_{\text{cm}}\phi_{\mathbf{K}}$  given by Eq. (46) simplifies as follows

$$\hat{H}_{\text{cm}}\phi_{\mathbf{K}} = \left[ \sum_{\nu=x,y}^2 \left[ \hbar\tilde{\omega} \left( \hat{c}_{\nu}^{\dagger}\hat{c}_{\nu} + \frac{1}{2} \right) - \frac{g^2}{\hbar\tilde{\omega}} (\mathbf{e}_{\nu} \cdot \mathbf{K})^2 \right] + \frac{\hbar^2 \mathbf{K}^2}{2m} \right] \phi_{\mathbf{K}}.$$

The operators defined in Eq. (47) also satisfy bosonic commutation relations  $[\hat{c}_{\nu}, \hat{c}_{\nu'}^{\dagger}] = \delta_{\nu\nu'}$  for  $\nu, \nu' = x, y$ . For the operator  $\hat{c}_{\nu}^{\dagger}\hat{c}_{\nu}$  the full set of eigenstates is [75]

$$|n_{\nu}, \mathbf{e}_{\nu} \cdot \mathbf{K}\rangle = \frac{(\hat{c}_{\nu}^{\dagger})^{n_{\nu}}}{\sqrt{n_{\nu}!}} |0_{\nu}, \mathbf{e}_{\nu} \cdot \mathbf{K}\rangle \quad \text{with } n_{\lambda} \in \mathbb{Z}, \nu = x, y, \quad (48)$$

where  $|0_{\nu}, \mathbf{e}_{\nu} \cdot \mathbf{K}\rangle$  is the ground state which gets annihilated by  $\hat{c}_{\nu}$  [75], and the spectrum of the bosonic operator  $\hbar\tilde{\omega}(\hat{c}_{\nu}^{\dagger}\hat{c}_{\nu} + 1/2)$  is  $\hbar\tilde{\omega}(n_{\nu} + 1/2)$ . Finally, applying  $\hat{H}_{\text{cm}}\phi_{\mathbf{K}}$  on the eigenstates  $\prod_{\nu} |n_{\nu}, \mathbf{e}_{\nu} \cdot \mathbf{K}\rangle$  of the bosonic part of the Hamiltonian we obtain

$$\begin{aligned} \hat{H}_{\text{cm}} \left[ \phi_{\mathbf{K}} \prod_{\nu=x,y}^2 |n_{\nu}, \mathbf{e}_{\nu} \cdot \mathbf{K}\rangle \right] = \\ \left( \sum_{\nu=x,y}^2 \left[ \hbar\tilde{\omega} \left( n_{\nu} + \frac{1}{2} \right) - \frac{g^2 (\mathbf{e}_{\nu} \cdot \mathbf{K})^2}{\hbar\tilde{\omega}} \right] + \frac{\hbar^2 \mathbf{K}^2}{2m} \right) \left[ \phi_{\mathbf{K}} \prod_{\nu=x,y}^2 |n_{\nu}, \mathbf{e}_{\nu} \cdot \mathbf{K}\rangle \right]. \end{aligned} \quad (49)$$

From the above expression we can deduce the exact light-matter eigenfunctions of the many-body system and the respective eigenspectrum. The solution exactly reproduces the solution obtained in Ref. [64] for the free electron gas.

## B Matter and Photon Operators in Terms of the Polaritonic Operators

In what follows we derive the expressions for the photon and matter operators in terms of the polaritonic operators.

### B.1 Photonic operators

The annihilation and creation operators  $\{\hat{a}_{\nu}, \hat{a}_{\nu}^{\dagger}\}$  of the photon field in terms of the displacement coordinate  $q_{\nu}$  and the conjugate momentum  $\partial_{q_{\nu}}$  are

$$\hat{a}_{\nu} = \frac{1}{\sqrt{2}} \left( q_{\nu} + \frac{\partial}{\partial q_{\nu}} \right) \quad \text{and} \quad \hat{a}_{\nu}^{\dagger} = \frac{1}{\sqrt{2}} \left( q_{\nu} - \frac{\partial}{\partial q_{\nu}} \right). \quad (50)$$

The coordinate  $q_{\nu}$  and its momentum are related to  $V_{\nu-}$  and  $\partial_{V_{\nu-}}$  via the relations

$$q_{\nu} = -\sqrt{\frac{\omega}{\hbar}} V_{\nu-} \quad \text{and} \quad \frac{\partial}{\partial q_{\nu}} = -\sqrt{\frac{\hbar}{\omega}} \frac{\partial}{\partial V_{\nu-}}. \quad (51)$$

Using the expressions  $S_{\nu l} = \sum_j O_{jl} V_{\nu j}$  and  $\partial/\partial S_{\nu l} = \sum_j O_{jl} \partial/\partial V_{\nu j}$ , we find  $V_{\nu-}$  and  $\partial_{V_{\nu-}}$  in terms of  $\{S_{\nu l}, \partial_{S_{\nu l}}\}$

$$V_{\nu-} = \frac{S_{\nu-} - \Lambda S_{\nu+}}{\sqrt{1 + \Lambda^2}} \quad \text{and} \quad \partial_{V_{\nu-}} = \frac{\partial_{S_{\nu-}} - \Lambda \partial_{S_{\nu+}}}{\sqrt{1 + \Lambda^2}}. \quad (52)$$

Then, the photonic displacement coordinate  $q_\nu$  and its conjugate momentum with respect to  $\{S_{\nu l}, \partial_{S_{\nu l}}\}$  read

$$q_\nu = -\frac{S_{\nu-} - \Lambda S_{\nu+}}{\sqrt{1 + \Lambda^2}} \sqrt{\frac{\omega}{\hbar}} \text{ and } \partial_{q_\nu} = -\frac{\partial_{S_{\nu-}} - \Lambda \partial_{S_{\nu+}}}{\sqrt{1 + \Lambda^2}} \sqrt{\frac{\hbar}{\omega}}. \quad (53)$$

The polariton annihilation and creation operators with regard to the polariton coordinates and momenta take the form

$$\hat{d}_{\nu l} = S_{\nu l} \sqrt{\frac{\Omega_l}{2\hbar}} + \sqrt{\frac{\hbar}{2\Omega_l}} \partial_{S_{\nu l}} \text{ and } \hat{d}_{\nu l}^\dagger = S_{\nu l} \sqrt{\frac{\Omega_l}{2\hbar}} - \sqrt{\frac{\hbar}{2\Omega_l}} \partial_{S_{\nu l}}. \quad (54)$$

By inverting the above equation we express  $S_{\nu l}$  and  $\partial_{S_{\nu l}}$  with respect to  $\{\hat{d}_{\nu l}, \hat{d}_{\nu l}^\dagger\}$

$$S_{\nu l} = \sqrt{\frac{\hbar}{2\Omega_l}} (\hat{d}_{\nu l}^\dagger + \hat{d}_{\nu l}) \text{ and } \partial_{S_{\nu l}} = \sqrt{\frac{\Omega_l}{2\hbar}} (\hat{d}_{\nu l} - \hat{d}_{\nu l}^\dagger). \quad (55)$$

Then, combining Eqs. (53) and (55) we obtain the expressions for the photonic operators  $\{\hat{a}_\nu, \hat{a}_\nu^\dagger\}$  in terms of the polaritonic ones  $\{\hat{d}_{\nu l}, \hat{d}_{\nu l}^\dagger\}$ , namely

$$\hat{a}_\nu = \frac{-1}{\sqrt{2 + 2\Lambda^2}} \left[ \frac{\omega + \Omega_-}{\sqrt{2\Omega_- \omega}} \hat{d}_{\nu-} + \frac{\omega - \Omega_-}{\sqrt{2\Omega_- \omega}} \hat{d}_{\nu-}^\dagger - \Lambda \left( \frac{\omega + \Omega_+}{\sqrt{2\omega\Omega_+}} \hat{d}_{\nu+} + \frac{\omega - \Omega_+}{\sqrt{2\omega\Omega_+}} \hat{d}_{\nu+}^\dagger \right) \right]. \quad (56)$$

Accordingly, the operator  $\hat{a}_\nu^\dagger$  is obtained by conjugation.

## B.2 Matter operators

The purely matter contribution  $\hat{H}_m$  of the CM Hamiltonian  $\hat{H}_{\text{cm}}$  is a sum of two uncoupled harmonic oscillators [Eq. (11)]. This can also be written in terms of the annihilation and creation operators as follows

$$\hat{H}_m = \sum_{\nu=x,y} -\frac{\hbar^2}{2m} \frac{\partial^2}{\partial R_\nu^2} + \frac{m\Omega^2}{2} R_\nu^2 = \sum_{\nu=x,y} \hbar\Omega \left( \hat{m}_\nu^\dagger \hat{m}_\nu + \frac{1}{2} \right), \quad (57)$$

where the operator

$$\hat{m}_\nu = R_\nu \sqrt{\frac{m\Omega}{2\hbar}} + \frac{\partial}{\partial R_\nu} \sqrt{\frac{\hbar}{2m\Omega}}, \quad (58)$$

and  $\hat{m}_\nu^\dagger$  its conjugate. Recall that in order to diagonalize the light-matter Hamiltonian in Sec. 3 we performed a Fourier transform on the matter coordinates. After the Fourier transformation the matter annihilation operator becomes

$$\hat{m}_\nu = i \frac{\partial}{\partial K_\nu} \sqrt{\frac{m\Omega}{2\hbar}} + i K_\nu \sqrt{\frac{\hbar}{2m\Omega}}. \quad (59)$$

Moreover, employing the relation between  $K_\nu = V_{\nu+} \sqrt{\hbar^2/m\Omega^2}$  and their conjugate momenta via the chain rule we have

$$\hat{m}_\nu = i \frac{\partial}{\partial V_{\nu+}} \sqrt{\frac{\hbar}{2\Omega}} + i V_{\nu+} \sqrt{\frac{\Omega}{2\hbar}}. \quad (60)$$

Additionally, using  $S_{\nu l} = \sum_j O_{jl} V_{\nu j}$  and  $\partial/\partial S_{\nu l} = \sum_j O_{jl} \partial/\partial V_{\nu j}$ , we find the expressions for  $V_{\nu+}$  and  $\partial_{V_{\nu+}}$  in terms of  $\{S_{\nu l}, \partial_{V_{\nu l}}\}$  i.e.

$$V_{\nu+} = \frac{\Lambda S_{\nu-} + S_{\nu+}}{\sqrt{1 + \Lambda^2}} \quad \text{and} \quad \partial_{V_{\nu+}} = \frac{\Lambda \partial_{S_{\nu-}} + \partial_{S_{\nu+}}}{\sqrt{1 + \Lambda^2}}. \quad (61)$$

Finally, with the use of Eq. (55) the expressions for the matter annihilation and creation operators with respect to the polaritonic ones are obtained. In particular

$$\hat{m}_\nu = \frac{i}{\sqrt{2 + 2\Lambda^2}} \left[ \Lambda \left( \frac{\Omega_- + \Omega}{\sqrt{2\Omega\Omega_-}} \hat{d}_{\nu-} + \frac{\Omega - \Omega_-}{\sqrt{2\Omega\Omega_-}} \hat{d}_{\nu-}^\dagger \right) + \frac{\Omega_+ + \Omega}{\sqrt{2\Omega_+\Omega}} \hat{d}_{\nu+} + \frac{\Omega - \Omega_+}{\sqrt{2\Omega_+\Omega}} \hat{d}_{\nu+}^\dagger \right], \quad (62)$$

where  $\hat{m}_\nu^\dagger$  can be determined through conjugation. Notice that by combining Eqs. (62) and (59) we can find the expression for the matter operators  $R_\nu$  and  $\partial_{R_\nu}$  in terms of the polaritonic ones.

## C Computation of the Four-Point Photon Function

Here, we elaborate on the calculation of the four-point function  $\langle \hat{a}_\nu^\dagger \hat{a}_\nu^\dagger \hat{a}_\nu \hat{a}_\nu \rangle_{\text{gs}}$  appearing in the Mandel  $Q$  parameter of Eq. (33). The photon operators in terms of the polaritonic ones are given by Eq. (30). In the four-point operator  $\hat{a}^\dagger \hat{a}^\dagger \hat{a} \hat{a}$  the terms that give non-zero contribution are:

$$\begin{aligned} & \hat{d}_{\nu-} \hat{d}_{\nu-} \hat{d}_{\nu-}^\dagger \hat{d}_{\nu-}^\dagger, \quad \hat{d}_{\nu+} \hat{d}_{\nu+} \hat{d}_{\nu+}^\dagger \hat{d}_{\nu+}^\dagger, \quad \hat{d}_{\nu-} \hat{d}_{\nu-}^\dagger \hat{d}_{\nu-} \hat{d}_{\nu-}^\dagger, \\ & \hat{d}_{\nu+} \hat{d}_{\nu+}^\dagger \hat{d}_{\nu+} \hat{d}_{\nu+}^\dagger, \quad \hat{d}_{\nu-} \hat{d}_{\nu-}^\dagger \hat{d}_{\nu+} \hat{d}_{\nu+}^\dagger, \quad \hat{d}_{\nu-} \hat{d}_{\nu+} \hat{d}_{\nu-}^\dagger \hat{d}_{\nu+}^\dagger, \\ & \hat{d}_{\nu+} \hat{d}_{\nu-} \hat{d}_{\nu-}^\dagger \hat{d}_{\nu+}^\dagger, \quad \hat{d}_{\nu+} \hat{d}_{\nu-} \hat{d}_{\nu+}^\dagger \hat{d}_{\nu-}^\dagger, \quad \hat{d}_{\nu+} \hat{d}_{\nu+}^\dagger \hat{d}_{\nu-} \hat{d}_{\nu-}^\dagger, \\ & \hat{d}_{\nu-} \hat{d}_{\nu+} \hat{d}_{\nu+}^\dagger \hat{d}_{\nu-}^\dagger. \end{aligned} \quad (63)$$

With this information we can obtain all the non-zero contributions in the four-point function

$$\begin{aligned} \langle \hat{a}_\nu^\dagger \hat{a}_\nu^\dagger \hat{a}_\nu \hat{a}_\nu \rangle_{\text{gs}} &= \frac{1}{(4 + 4\Lambda^2)^2} \left[ \frac{(\Omega_- - \omega)^4}{\omega^2 \Omega_-^2} \langle \hat{d}_{\nu-} \hat{d}_{\nu-} \hat{d}_{\nu-}^\dagger \hat{d}_{\nu-}^\dagger \rangle_{\text{gs}} \right. \\ &+ \frac{\Lambda^4 (\Omega_+ - \omega)^4}{\omega^2 \Omega_+^2} \langle \hat{d}_{\nu+} \hat{d}_{\nu+} \hat{d}_{\nu+}^\dagger \hat{d}_{\nu+}^\dagger \rangle_{\text{gs}} + \frac{\Lambda^4 (\Omega_+ - \omega)^2 (\Omega_+ + \omega)^2}{\omega^2 \Omega_+^2} \langle \hat{d}_{\nu+} \hat{d}_{\nu+}^\dagger \hat{d}_{\nu+} \hat{d}_{\nu+}^\dagger \rangle_{\text{gs}} + \\ &+ \frac{\Lambda^2 (\Omega_-^2 - \omega^2) (\Omega_+^2 - \omega^2)}{\omega^2 \Omega_+ \Omega_-} (\langle \hat{d}_{\nu-} \hat{d}_{\nu-}^\dagger \hat{d}_{\nu+} \hat{d}_{\nu+}^\dagger \rangle_{\text{gs}} + \langle \hat{d}_{\nu+} \hat{d}_{\nu+}^\dagger \hat{d}_{\nu-} \hat{d}_{\nu-}^\dagger \rangle_{\text{gs}}) \\ &+ \frac{\Lambda^2 (\Omega_+ - \omega)^2 (\Omega_- - \omega)^2}{\omega^2 \Omega_+ \Omega_-} (\langle \hat{d}_{\nu-} \hat{d}_{\nu+} \hat{d}_{\nu-}^\dagger \hat{d}_{\nu+}^\dagger \rangle_{\text{gs}} + \langle \hat{d}_{\nu+} \hat{d}_{\nu-} \hat{d}_{\nu-}^\dagger \hat{d}_{\nu+}^\dagger \rangle_{\text{gs}} + \langle \hat{d}_{\nu+} \hat{d}_{\nu+} \hat{d}_{\nu+}^\dagger \hat{d}_{\nu-}^\dagger \rangle_{\text{gs}}) \\ &+ \left. \frac{\Lambda^2 (\Omega_+ - \omega)^2 (\Omega_- - \omega)^2}{\omega^2 \Omega_+ \Omega_-} \langle \hat{d}_{\nu-} \hat{d}_{\nu+} \hat{d}_{\nu+}^\dagger \hat{d}_{\nu-}^\dagger \rangle_{\text{gs}} + \frac{(\Omega_- - \omega)^2 (\Omega_- + \omega)^2}{\omega^2 \Omega_-^2} \langle \hat{d}_{\nu-} \hat{d}_{\nu-}^\dagger \hat{d}_{\nu-} \hat{d}_{\nu-}^\dagger \rangle_{\text{gs}} \right]. \end{aligned} \quad (64)$$

Using the bosonic algebra of the polariton operators we find the following expression for the four-point function

$$\begin{aligned} \langle \hat{a}_\nu^\dagger \hat{a}_\nu^\dagger \hat{a}_\nu \hat{a}_\nu \rangle_{\text{gs}} &= \frac{1}{(4 + 4\Lambda^2)^2} \left[ \frac{2(\Omega_- - \omega)^4}{\omega^2 \Omega_-^2} + \frac{(\Omega_-^2 - \omega^2)^2}{\omega^2 \Omega_-^2} + \frac{2\Lambda^4 (\Omega_+ - \omega)^4}{\omega^2 \Omega_+^2} \right. \\ &+ \left. \frac{\Lambda^4 (\Omega_+^2 - \omega^2)^2}{\omega^2 \Omega_+^2} + \frac{2\Lambda^2 (\Omega_-^2 - \omega^2) (\Omega_+^2 - \omega^2)}{\omega^2 \Omega_+ \Omega_-} + \frac{4\Lambda^2 (\Omega_+ - \omega)^2 (\Omega_- - \omega)^2}{\omega^2 \Omega_+ \Omega_-} \right]. \end{aligned} \quad (65)$$

In the last step we also used that  $(\Omega_\pm - \omega)(\Omega_\pm + \omega) = \Omega_\pm^2 - \omega^2$ .

---

## References

- [1] M. Ruggenthaler, N. Tancogne-Dejean, J. Flick, H. Appel and A. Rubio, *From a quantum-electrodynamical light–matter description to novel spectroscopies*, Nat. Rev. Chem. **2**(3), 0118 (2018), doi:[10.1038/s41570-018-0118](https://doi.org/10.1038/s41570-018-0118).
- [2] F. Schlawin, D. M. Kennes and M. A. Sentef, *Cavity quantum materials*, Appl. Phys. Rev. **9**(1), 011312 (2022), doi:[10.1063/5.0083825](https://doi.org/10.1063/5.0083825).
- [3] F. J. Garcia-Vidal, C. Ciuti and T. W. Ebbesen, *Manipulating matter by strong coupling to vacuum fields*, Science **373**(6551), eabd0336 (2021), doi:[10.1126/science.abd0336](https://doi.org/10.1126/science.abd0336).
- [4] C. Cohen-Tannoudji, J. Dupont-Roc and G. Grynberg, *Photons and Atoms-Introduction to Quantum Electrodynamics*, Wiley-VCH (1997).
- [5] T. W. Ebbesen, *Hybrid light–matter states in a molecular and material science perspective*, Acc. Chem. Res. **49**(11), 2403 (2016), doi:[10.1021/acs.accounts.6b00295](https://doi.org/10.1021/acs.accounts.6b00295).
- [6] J. George, T. Chervy, A. Shalabney, E. Devaux, H. Hiura, C. Genet and T. W. Ebbesen, *Multiple rabi splittings under ultrastrong vibrational coupling*, Phys. Rev. Lett. **117**, 153601 (2016), doi:[10.1103/PhysRevLett.117.153601](https://doi.org/10.1103/PhysRevLett.117.153601).
- [7] J. Hutchison, A. Liscio, T. Schwartz, A. Canaguier-Durand, C. Genet, V. Palermo, P. Samorì and T. W. Ebbesen, *Tuning the work-function via strong coupling*, Adv. Mater. **25**(17), 2481 (2013), doi:[10.1002/adma.201203682](https://doi.org/10.1002/adma.201203682).
- [8] J. A. Hutchison, T. Schwartz, C. Genet, E. Devaux and T. W. Ebbesen, *Modifying chemical landscapes by coupling to vacuum fields*, Angew. Chem. Int. Ed. **51**(7), 1592 (2012), doi:[10.1002/anie.201107033](https://doi.org/10.1002/anie.201107033).
- [9] E. Orgiu, J. George, J. A. Hutchison, E. Devaux, J. F. Dayen, B. Doudin, F. Stellacci, C. Genet, J. Schachenmayer, C. Genes, G. Pupillo, P. Samorì *et al.*, *Conductivity in organic semiconductors hybridized with the vacuum field*, Nat. Mater. **14**(11), 1123 (2015), doi:[10.1038/nmat4392](https://doi.org/10.1038/nmat4392).
- [10] J. Feist, J. Galego and F. J. Garcia-Vidal, *Polaritonic chemistry with organic molecules*, ACS Photonics **5**(1), 205 (2017), doi:[10.1021/acsphotonics.7b00680](https://doi.org/10.1021/acsphotonics.7b00680).
- [11] J. Galego, F. J. Garcia-Vidal and J. Feist, *Suppressing photochemical reactions with quantized light fields*, Nat. Commun. **7**, 13841 (2016), doi:[10.1038/ncomms13841](https://doi.org/10.1038/ncomms13841).
- [12] C. Schäfer, M. Ruggenthaler, H. Appel and A. Rubio, *Modification of excitation and charge transfer in cavity quantum-electrodynamical chemistry*, PNAS **116**(11), 4883 (2019), doi:[10.1073/pnas.1814178116](https://doi.org/10.1073/pnas.1814178116).
- [13] T. E. Li, A. Nitzan and J. E. Subotnik, *On the origin of ground-state vacuum-field catalysis: Equilibrium consideration*, arXiv:2002.09977 [physics.chem-ph] (2020).
- [14] F. Mivehvar, F. Piazza, T. Donner and H. Ritsch, *Cavity qed with quantum gases: new paradigms in many-body physics*, Adv. Phys. **70**(1), 1 (2021), doi:[10.1080/00018732.2021.1969727](https://doi.org/10.1080/00018732.2021.1969727).

- 
- [15] Basov, D. N., Averitt, R. D. and Hsieh, D., *Towards properties on demand in quantum materials*, Nature Materials **16**(11), 1077 (2017), doi:[10.1209/epl/i2005-10344-3](https://doi.org/10.1209/epl/i2005-10344-3).
- [16] M. Buzzi, M. Först, M. Sigrist, R. Mankowsky and A. Cavalleri, *Probing dynamics in quantum materials with femtosecond X-rays*, Nat. Rev. Mat. **3**, 299 (2018), doi:[10.1038/s41578-018-0024-9](https://doi.org/10.1038/s41578-018-0024-9).
- [17] X. Wang, E. Ronca and M. A. Sentef, *Cavity quantum electrodynamical Chern insulator: Towards light-induced quantized anomalous Hall effect in graphene*, Phys. Rev. B **99**, 235156 (2019), doi:[10.1103/PhysRevB.99.235156](https://doi.org/10.1103/PhysRevB.99.235156).
- [18] M. Kiffner, J. R. Coulthard, F. Schlawin, A. Ardavan and D. Jaksch, *Manipulating quantum materials with quantum light*, Phys. Rev. B **99**, 085116 (2019), doi:[10.1103/PhysRevB.99.085116](https://doi.org/10.1103/PhysRevB.99.085116).
- [19] J. Li, D. Golez, G. Mazza, A. J. Millis, A. Georges and M. Eckstein, *Electromagnetic coupling in tight-binding models for strongly correlated light and matter*, Phys. Rev. B **101**, 205140 (2020), doi:[10.1103/PhysRevB.101.205140](https://doi.org/10.1103/PhysRevB.101.205140).
- [20] Y. Ashida, A. m. c. İmamoğlu and E. Demler, *Cavity quantum electrodynamics at arbitrary light-matter coupling strengths*, Phys. Rev. Lett. **126**, 153603 (2021), doi:[10.1103/PhysRevLett.126.153603](https://doi.org/10.1103/PhysRevLett.126.153603).
- [21] A. F. Kockum, A. Miranowicz, S. De Liberato, S. Savasta and F. Nori, *Ultrastrong coupling between light and matter*, Nat. Rev. Phys. **1**(1), 19 (2019).
- [22] P. Forn-Díaz, L. Lamata, E. Rico, J. Kono and E. Solano, *Ultrastrong coupling regimes of light-matter interaction*, Rev. Mod. Phys. **91**, 025005 (2019), doi:[10.1103/RevModPhys.91.025005](https://doi.org/10.1103/RevModPhys.91.025005).
- [23] D. N. Basov, A. Asenjo-Garcia, P. J. Schuck, X. Zhu and A. Rubio, *Polariton panorama*, Nanophotonics **10**(1), 549 (2021), doi:[doi:10.1515/nanoph-2020-0449](https://doi.org/10.1515/nanoph-2020-0449).
- [24] I. Carusotto and C. Ciuti, *Quantum fluids of light*, Rev. Mod. Phys. **85**, 299 (2013), doi:[10.1103/RevModPhys.85.299](https://doi.org/10.1103/RevModPhys.85.299).
- [25] D. Sidler, M. Ruggenthaler, C. Schäfer, E. Ronca and A. Rubio, *A perspective on ab initio modeling of polaritonic chemistry: The role of non-equilibrium effects and quantum collectivity*, J. Chem. Phys. **156**(23), 230901 (2022), doi:[10.1063/5.0094956](https://doi.org/10.1063/5.0094956).
- [26] J. Flick, M. Ruggenthaler, H. Appel and A. Rubio, *Atoms and molecules in cavities, from weak to strong coupling in quantum-electrodynamics (QED) chemistry*, PNAS **114**(12), 3026 (2017), doi:[10.1073/pnas.1615509114](https://doi.org/10.1073/pnas.1615509114).
- [27] S. Latini, E. Ronca, U. De Giovannini, H. Hübener and A. Rubio, *Cavity control of excitons in two-dimensional materials*, Nano Lett. **19**, 3473 (2019), doi:[10.1021/acs.nanolett.9b00183](https://doi.org/10.1021/acs.nanolett.9b00183).
- [28] M. Förg, L. Colombier, R. K. Patel, J. Lindlau, A. D. Mohite, H. Yamaguchi, M. M. Glazov, D. Hunger and A. Högele, *Cavity-control of interlayer excitons in Van der Waals heterostructures*, Nat. Commun. **10**, 3697 (2019), doi:[10.1038/s41467-019-11620-z](https://doi.org/10.1038/s41467-019-11620-z).

- 
- [29] J. Kasprzak, M. Richard, S. Kundermann, A. Baas, P. Jeambrun, J. M. J. Keeling, F. M. Marchetti, M. H. Szymańska, R. André, J. L. Staehli, V. Savona, P. B. Littlewood *et al.*, *Bose–Einstein condensation of exciton polaritons*, *Nature* **443**(7110), 409 (2006), doi:[10.1038/nature05131](https://doi.org/10.1038/nature05131).
- [30] J. Keeling and S. Kena-Cohen, *Bose–Einstein condensation of exciton-polaritons in organic microcavities*, *Ann. Rev. Phys. Chem.* **71**(1), 435 (2020), doi:[10.1146/annurev-physchem-010920-102509](https://doi.org/10.1146/annurev-physchem-010920-102509).
- [31] F. Schlawin, A. Cavalleri and D. Jaksch, *Cavity-mediated electron-photon superconductivity*, *Phys. Rev. Lett.* **122**, 133602 (2019), doi:[10.1103/PhysRevLett.122.133602](https://doi.org/10.1103/PhysRevLett.122.133602).
- [32] O. Cotlet, S. Zeytinoğlu, M. Sigrist, E. Demler and A. Imamoglu, *Superconductivity and other collective phenomena in a hybrid bose-fermi mixture formed by a polariton condensate and an electron system in two dimensions*, *Phys. Rev. B* **93**, 054510 (2016), doi:[10.1103/PhysRevB.93.054510](https://doi.org/10.1103/PhysRevB.93.054510).
- [33] M. A. Sentef, M. Ruggenthaler and A. Rubio, *Cavity quantum-electrodynamical polaritonically enhanced electron-phonon coupling and its influence on superconductivity*, *Sci. Adv.* **4**(11), eaau6969 (2018).
- [34] J. B. Curtis, Z. M. Raines, A. A. Allocca, M. Hafezi and V. M. Galitski, *Cavity quantum Eliashberg enhancement of superconductivity*, *Phys. Rev. Lett.* **122**, 167002 (2019), doi:[10.1103/PhysRevLett.122.167002](https://doi.org/10.1103/PhysRevLett.122.167002).
- [35] A. Thomas, E. Devaux, K. Nagarajan, T. Chervy, M. Seidel, D. Hagenmüller, S. Schütz, J. Schachenmayer, C. Genet, G. Pupillo and T. W. Ebbesen, *Exploring superconductivity under strong coupling with the vacuum electromagnetic field*, arXiv:1911.01459 [cond-mat.supr-con] (2019).
- [36] H. Hübener, U. De Giovannini, C. Schäfer, J. Andberger, M. Ruggenthaler, J. Faist and A. Rubio, *Engineering quantum materials with chiral optical cavities*, *Nat. Mater.* **20**, 438 (2021), doi:[10.1038/s41563-020-00801-7](https://doi.org/10.1038/s41563-020-00801-7).
- [37] J. Petersen, J. Volz and A. Rauschenbeutel, *Chiral nanophotonic waveguide interface based on spin-orbit interaction of light*, *Science* **346**(6205), 67 (2014), doi:[10.1126/science.1257671](https://doi.org/10.1126/science.1257671).
- [38] F. Zhang, J. Ren, L. Shan, X. Duan, Y. Li, T. Zhang, Q. Gong and Y. Gu, *Chiral cavity quantum electrodynamics with coupled nanophotonic structures*, *Phys. Rev. A* **100**, 053841 (2019), doi:[10.1103/PhysRevA.100.053841](https://doi.org/10.1103/PhysRevA.100.053841).
- [39] P. Lodahl, S. Mahmoodian, S. Stobbe, A. Rauschenbeutel, P. Schneeweiss, J. Volz, H. Pichler and P. Zoller, *Chiral quantum optics*, *Nature* **541**, 473 (2017), doi:[10.1038/nature21037](https://doi.org/10.1038/nature21037).
- [40] S. Latini, D. Shin, S. A. Sato, C. Schäfer, U. De Giovannini, H. Hübener and A. Rubio, *The ferroelectric photo-groundstate of SrTiO<sub>3</sub>: Cavity materials engineering*, arXiv:2101.11313 [cond-mat.mtrl-sci] (2021).
- [41] Y. Ashida, A. Imamoglu, J. Faist, D. Jaksch, A. Cavalleri and E. Demler, *Quantum electrodynamic control of matter: Cavity-enhanced ferroelectric phase transition*, *Phys. Rev. X* **10**, 041027 (2020), doi:[10.1103/PhysRevX.10.041027](https://doi.org/10.1103/PhysRevX.10.041027).

- 
- [42] J. Keller, G. Scalari, F. Appugliese, S. Rajabali, M. Beck, J. Haase, C. A. Lehner, W. Wegscheider, M. Failla, M. Myronov, D. R. Leadley, J. Lloyd-Hughes *et al.*, *Landau polaritons in highly nonparabolic two-dimensional gases in the ultrastrong coupling regime*, Phys. Rev. B **101**, 075301 (2020), doi:[10.1103/PhysRevB.101.075301](https://doi.org/10.1103/PhysRevB.101.075301).
- [43] G. Scalari, C. Maissen, D. Turčinková, D. Hagenmüller, S. De Liberato, C. Ciuti, C. Reichl, D. Schuh, W. Wegscheider, M. Beck and J. Faist, *Ultrastrong coupling of the cyclotron transition of a 2D electron gas to a THz metamaterial*, Science **335**(6074), 1323 (2012), doi:[10.1126/science.1216022](https://doi.org/10.1126/science.1216022).
- [44] X. Li, M. Bamba, Q. Zhang, S. Fallahi, G. C. Gardner, W. Gao, M. Lou, K. Yoshioka, M. J. Manfra and J. Kono, *Vacuum Bloch–Siegert shift in Landau polaritons with ultra-high cooperativity*, Nature Photon. **12**, 324 (2018), doi:[10.1038/s41566-018-0153-0](https://doi.org/10.1038/s41566-018-0153-0).
- [45] A. Bayer, M. Pozimski, S. Schambeck, D. Schuh, R. Huber, D. Bougeard and C. Lange, *Terahertz light–matter interaction beyond unity coupling strength*, Nano Lett. **17**(10), 6340 (2017), doi:[10.1021/acs.nanolett.7b03103](https://doi.org/10.1021/acs.nanolett.7b03103), PMID: 28937772.
- [46] S. Ravets, P. Knüppel, S. Faelt, O. Cotlet, M. Kroner, W. Wegscheider and A. Imamoglu, *Polaron polaritons in the integer and fractional quantum Hall regimes*, Phys. Rev. Lett. **120**, 057401 (2018), doi:[10.1103/PhysRevLett.120.057401](https://doi.org/10.1103/PhysRevLett.120.057401).
- [47] S. Smolka, W. Wuester, F. Haupt, S. Faelt, W. Wegscheider and A. Imamoglu, *Cavity quantum electrodynamics with many-body states of a two-dimensional electron gas*, Science **346**(6207), 332 (2014), doi:[10.1126/science.1258595](https://doi.org/10.1126/science.1258595).
- [48] G. L. Paravicini-Bagliani, F. Appugliese, E. Richter, S. Fallahi, F. Valmorra, J. Keller, M. Beck, N. Bartolo, C. Rössler, T. Ihn, K. Ensslin, C. Ciuti *et al.*, *Magneto-transport controlled by Landau polariton states*, Nat. Phys. **15**, 186 (2019), doi:[10.1038/s41567-018-0346-y](https://doi.org/10.1038/s41567-018-0346-y).
- [49] D. Hagenmüller, S. De Liberato and C. Ciuti, *Ultrastrong coupling between a cavity resonator and the cyclotron transition of a two-dimensional electron gas in the case of an integer filling factor*, Phys. Rev. B **81**, 235303 (2010), doi:[10.1103/PhysRevB.81.235303](https://doi.org/10.1103/PhysRevB.81.235303).
- [50] V. Rokaj, M. Penz, M. A. Sentef, M. Ruggenthaler and A. Rubio, *Quantum electrodynamical Bloch theory with homogeneous magnetic fields*, Phys. Rev. Lett. **123**, 047202 (2019), doi:[10.1103/PhysRevLett.123.047202](https://doi.org/10.1103/PhysRevLett.123.047202).
- [51] C. Ciuti, *Cavity-mediated electron hopping in disordered quantum hall systems*, Phys. Rev. B **104**, 155307 (2021), doi:[10.1103/PhysRevB.104.155307](https://doi.org/10.1103/PhysRevB.104.155307).
- [52] V. Rokaj, M. Penz, M. A. Sentef, M. Ruggenthaler and A. Rubio, *Polaritonic hofstadter butterfly and cavity control of the quantized hall conductance*, Phys. Rev. B **105**, 205424 (2022), doi:[10.1103/PhysRevB.105.205424](https://doi.org/10.1103/PhysRevB.105.205424).
- [53] F. Appugliese, J. Enkner, G. L. Paravicini-Bagliani, M. Beck, C. Reichl, W. Wegscheider, G. Scalari, C. Ciuti and J. Faist, *Breakdown of topological protection by cavity vacuum fields in the integer quantum Hall effect*, Science **375**(6584), 1030 (2022), doi:[10.1126/science.abl5818](https://doi.org/10.1126/science.abl5818).



- 
- [54] I. V. Tokatly, *Time-dependent density functional theory for many-electron systems interacting with cavity photons*, Phys. Rev. Lett. **110**, 233001 (2013), doi:[10.1103/PhysRevLett.110.233001](https://doi.org/10.1103/PhysRevLett.110.233001).
- [55] M. Ruggenthaler, J. Flick, C. Pellegrini, H. Appel, I. V. Tokatly and A. Rubio, *Quantum-electrodynamical density-functional theory: Bridging quantum optics and electronic-structure theory*, Phys. Rev. A **90**, 012508 (2014), doi:[10.1103/PhysRevA.90.012508](https://doi.org/10.1103/PhysRevA.90.012508).
- [56] C. Pellegrini, J. Flick, I. V. Tokatly, H. Appel and A. Rubio, *Optimized effective potential for quantum electrodynamic time-dependent density functional theory*, Phys. Rev. Lett. **115**, 093001 (2015), doi:[10.1103/PhysRevLett.115.093001](https://doi.org/10.1103/PhysRevLett.115.093001).
- [57] F. Buchholz, I. Theophilou, M. Giesbertz, K. J. H. and Ruggenthaler and A. Rubio, *Light-matter hybrid-orbital-based first-principles methods: The influence of polariton statistics*, J. Chem. Th. and Comp. **16**, 5601 (2020), doi:[doi: 10.1021/acs.jctc.0c00469](https://doi.org/10.1021/acs.jctc.0c00469).
- [58] T. S. Haugland, E. Ronca, E. F. Kjørstad, A. Rubio and H. Koch, *Coupled cluster theory for molecular polaritons: Changing ground and excited states*, Phys. Rev. X **10**, 041043 (2020), doi:[10.1103/PhysRevX.10.041043](https://doi.org/10.1103/PhysRevX.10.041043).
- [59] U. Mordovina, C. Bungey, H. Appel, P. J. Knowles, A. Rubio and F. R. Manby, *Polaritonic coupled-cluster theory*, Phys. Rev. Research **2**, 023262 (2020), doi:[10.1103/PhysRevResearch.2.023262](https://doi.org/10.1103/PhysRevResearch.2.023262).
- [60] G. D. Mahan, *Many Particle Physics*, Springer, New York (2010).
- [61] V. Rokaj, D. M. Welakuh, M. Ruggenthaler and A. Rubio, *Light-matter interaction in the long-wavelength limit: no ground-state without dipole self-energy*, J. Phys. B: At. Mol. Opt. Phys. **51**(3), 034005 (2018).
- [62] F. H. Faisal, *Theory of Multiphoton Processes*, Springer, Berlin (1987).
- [63] M. Tomza, K. Jachymski, R. Gerritsma, A. Negretti, T. Calarco, Z. Idziaszek and P. S. Julienne, *Cold hybrid ion-atom systems*, Rev. Mod. Phys. **91**(3), 035001 (2019).
- [64] V. Rokaj, M. Ruggenthaler, F. G. Eich and A. Rubio, *Free electron gas in cavity quantum electrodynamics*, Phys. Rev. Research **4**, 013012 (2022), doi:[10.1103/PhysRevResearch.4.013012](https://doi.org/10.1103/PhysRevResearch.4.013012).
- [65] L. Mandel, *Sub-poissonian photon statistics in resonance fluorescence*, Opt. Lett. **4**(7), 205 (1979), doi:[10.1364/OL.4.000205](https://doi.org/10.1364/OL.4.000205).
- [66] F. Schlawin, A. Cavalleri and D. Jaksch, *Cavity-mediated electron-photon superconductivity*, Phys. Rev. Lett. **122**, 133602 (2019), doi:[10.1103/PhysRevLett.122.133602](https://doi.org/10.1103/PhysRevLett.122.133602).
- [67] D. M. Welakuh, M. Ruggenthaler, M.-L. M. Tchenkoue, H. Appel and A. Rubio, *Down-conversion processes in ab initio nonrelativistic quantum electrodynamics*, Phys. Rev. Research **3**, 033067 (2021), doi:[10.1103/PhysRevResearch.3.033067](https://doi.org/10.1103/PhysRevResearch.3.033067).
- [68] X. Li, A. Mandal and P. Huo, *Cavity frequency-dependent theory for vibrational polariton chemistry*, Nature Communications **12**, 1315 (2021), doi:[10.1038/s41467-021-21610-9](https://doi.org/10.1038/s41467-021-21610-9).

- 
- [69] C. Schäfer, J. Flick, E. Ronca, P. Narang and A. Rubio, *Shining light on the microscopic resonant mechanism responsible for cavity-mediated chemical reactivity*, doi:[10.48550/ARXIV.2104.12429](https://doi.org/10.48550/ARXIV.2104.12429) (2021).
- [70] K. Hepp and E. H. Lieb, *On the superradiant phase transition for molecules in a quantized radiation field: the Dicke maser model*, Ann. Phys. **76**(2), 360 (1973).
- [71] P. Nataf and C. Ciuti, *No-go theorem for superradiant quantum phase transitions in cavity QED and counter-example in circuit QED*, Nat. Comm. **1** (2010), doi:[10.1038/ncomms1069](https://doi.org/10.1038/ncomms1069).
- [72] C. Zener and R. H. Fowler, *Non-adiabatic crossing of energy levels*, Proceedings of the Royal Society of London. Series A, Containing Papers of a Mathematical and Physical Character **137**(833), 696 (1932), doi:[10.1098/rspa.1932.0165](https://doi.org/10.1098/rspa.1932.0165).
- [73] H. Spohn, *Dynamics of Charged Particles and their Radiation Field*, Cambridge university press (2004).
- [74] W. Greiner and J. Reinhardt, *Field Quantization*, Springer (1996).
- [75] D. J. Griffiths, *Introduction to Quantum Mechanics*, Prentice Hall (1995).
- [76] J. Malave, Y. S. Aklilu, M. Beutel, C. Huang and K. Varga, *Harmonically confined  $n$ -electron systems coupled to light in a cavity*, Phys. Rev. B **105**, 115127 (2022), doi:[10.1103/PhysRevB.105.115127](https://doi.org/10.1103/PhysRevB.105.115127).
- [77] W. Kohn, *Cyclotron resonance and de haas-van alphen oscillations of an interacting electron gas*, Phys. Rev. **123**, 1242 (1961), doi:[10.1103/PhysRev.123.1242](https://doi.org/10.1103/PhysRev.123.1242).
- [78] V. Rokaj, S. I. Mistakidis and H. R. Sadeghpour, [In preparation] (2022).
- [79] Y. Todorov, A. M. Andrews, R. Colombelli, S. De Liberato, C. Ciuti, P. Klang, G. Strasser and C. Sirtori, *Ultrastrong light-matter coupling regime with polariton dots*, Phys. Rev. Lett. **105**, 196402 (2010), doi:[10.1103/PhysRevLett.105.196402](https://doi.org/10.1103/PhysRevLett.105.196402).
- [80] Y. Todorov and C. Sirtori, *Intersubband polaritons in the electrical dipole gauge*, Phys. Rev. B **85**, 045304 (2012), doi:[10.1103/PhysRevB.85.045304](https://doi.org/10.1103/PhysRevB.85.045304).
- [81] Y. Todorov, *Dipolar quantum electrodynamics of the two-dimensional electron gas*, Phys. Rev. B **91**, 125409 (2015), doi:[10.1103/PhysRevB.91.125409](https://doi.org/10.1103/PhysRevB.91.125409).
- [82] R. F. Ribeiro, J. A. Campos-Gonzalez-Angulo, N. C. Giebink, W. Xiong and J. Yuen-Zhou, *Enhanced optical nonlinearities under collective strong light-matter coupling*, Phys. Rev. A **103**, 063111 (2021), doi:[10.1103/PhysRevA.103.063111](https://doi.org/10.1103/PhysRevA.103.063111).
- [83] R. H. Dicke, *Coherence in spontaneous radiation processes*, Phys. Rev. **93**, 99 (1954), doi:[10.1103/PhysRev.93.99](https://doi.org/10.1103/PhysRev.93.99).
- [84] B. M. Garraway, *The Dicke model in quantum optics: Dicke model revisited*, Phil. Trans. R. Soc. A **369**(1939), 1137 (2011), doi:[10.1098/rsta.2010.0333](https://doi.org/10.1098/rsta.2010.0333).
- [85] S. A. Ponomarenko, *Quantum harmonic oscillator revisited: A fourier transform approach*, American Journal of Physics **72**(9), 1259 (2004), doi:[10.1119/1.1677395](https://doi.org/10.1119/1.1677395).

- 
- [86] E. M. Purcell, *Spontaneous Emission Probabilities at Radio Frequencies*, Phys. Rev. **69**, 681 (1946), doi:[10.1103/PhysRev.69.674.2](https://doi.org/10.1103/PhysRev.69.674.2).
- [87] X. Li, M. Bamba, N. Yuan, Q. Zhang, Y. Zhao, M. Xiang, K. Xu, Z. Jin, W. Ren, G. Ma, S. Cao, D. Turchinovich *et al.*, *Observation of dicke cooperativity in magnetic interactions*, Science **361**(6404), 794 (2018), doi:[10.1126/science.aat5162](https://doi.org/10.1126/science.aat5162).
- [88] N. Fayard, L. Henriot, A. Asenjo-Garcia and D. E. Chang, *Many-body localization in waveguide quantum electrodynamics*, Phys. Rev. Research **3**, 033233 (2021), doi:[10.1103/PhysRevResearch.3.033233](https://doi.org/10.1103/PhysRevResearch.3.033233).
- [89] F. Scazza, M. Zaccanti, P. Massignan, M. M. Parish and J. Levinsen, *Repulsive fermi and bose polarons in quantum gases*, Atoms **10**(2), 55 (2022).
- [90] S. I. Mistakidis, G. M. Koutentakis, F. Grusdt, P. Schmelcher and H. R. Sadeghpour, *Inducing spin-order with an impurity: phase diagram of the magnetic bose polaron*, arXiv:2204.10960 (2022).
- [91] P. Massignan, M. Zaccanti and G. M. Bruun, *Polarons, dressed molecules and itinerant ferromagnetism in ultracold fermi gases*, Rep. Progr. Phys. **77**(3), 034401 (2014).
- [92] S. I. Mistakidis, A. G. Volosniev, R. E. Barfknecht, T. Fogarty, T. Busch, A. Foerster, P. Schmelcher and N. T. Zinner, *Cold atoms in low dimensions—a laboratory for quantum dynamics*, arXiv preprint arXiv:2202.11071 (2022).
- [93] S. I. Mistakidis, G. C. Katsimiga, G. M. Koutentakis, T. Busch and P. Schmelcher, *Quench dynamics and orthogonality catastrophe of bose polarons*, Phys. Rev. Lett. **122**, 183001 (2019), doi:[10.1103/PhysRevLett.122.183001](https://doi.org/10.1103/PhysRevLett.122.183001).
- [94] C. Schäfer, F. Buchholz, M. Penz, M. Ruggenthaler and A. Rubio, *Making ab initio qed functional(s): Nonperturbative and photon-free effective frameworks for strong light-matter coupling*, PNAS **118**(41), e2110464118 (2021), doi:[10.1073/pnas.2110464118](https://doi.org/10.1073/pnas.2110464118).
- [95] F. Schlawin, K. E. Dorfman and S. Mukamel, *Detection of photon statistics and multi-mode field correlations by raman processes*, J. Chem. Phys. **154**(10), 104116 (2021), doi:[10.1063/5.0039759](https://doi.org/10.1063/5.0039759).
- [96] P. Stegmann, S. N. Gupta, G. Haran and J. Cao, *Higher-order photon statistics as a new tool to reveal hidden excited states in a plasmonic cavity*, ACS Photonics **9**(6), 2119 (2022), doi:[10.1021/acsp Photonics.2c00375](https://doi.org/10.1021/acsp Photonics.2c00375).
- [97] A. Vukics, T. Grieser and P. Domokos, *Elimination of the A-square problem from cavity QED*, Phys. Rev. Lett. **112**, 073601 (2014), doi:[10.1103/PhysRevLett.112.073601](https://doi.org/10.1103/PhysRevLett.112.073601).
- [98] C. Schäfer, M. Ruggenthaler, V. Rokaj and A. Rubio, *Relevance of the quadratic diamagnetic and self-polarization terms in cavity quantum electrodynamics*, arXiv:1911.08427 [quant-ph] (2019).
- [99] D. De Bernardis, P. Pilar, T. Jaako, S. De Liberato and P. Rabl, *Breakdown of gauge invariance in ultrastrong-coupling cavity QED*, Phys. Rev. A **98**(5), 053819 (2018).

- 
- [100] O. Di Stefano, A. Settineri, V. Macrì, L. Garziano, R. Stassi, S. Savasta and F. Nori, *Resolution of gauge ambiguities in ultrastrong-coupling cavity quantum electrodynamics*, Nature Physics (2019).
- [101] I. Bialynicki-Birula and K. Rzażewski, *No-go theorem concerning the superradiant phase transition in atomic systems*, Phys. Rev. A **19**, 301 (1979), doi:[10.1103/PhysRevA.19.301](https://doi.org/10.1103/PhysRevA.19.301).
- [102] D. Hagenmüller and C. Ciuti, *Cavity QED of the graphene cyclotron transition*, Phys. Rev. Lett. **109**, 267403 (2012), doi:[10.1103/PhysRevLett.109.267403](https://doi.org/10.1103/PhysRevLett.109.267403).
- [103] G. Mazza and A. Georges, *Superradiant quantum materials*, Phys. Rev. Lett. **122**, 017401 (2019), doi:[10.1103/PhysRevLett.122.017401](https://doi.org/10.1103/PhysRevLett.122.017401).
- [104] O. Viehmann, J. von Delft and F. Marquardt, *Superradiant phase transitions and the standard description of circuit QED*, Phys. Rev. Lett. **107**, 113602 (2011), doi:[10.1103/PhysRevLett.107.113602](https://doi.org/10.1103/PhysRevLett.107.113602).
- [105] L. Chirolli, M. Polini, V. Giovannetti and A. H. MacDonald, *Drude weight, cyclotron resonance, and the Dicke model of graphene cavity QED*, Phys. Rev. Lett. **109**, 267404 (2012), doi:[10.1103/PhysRevLett.109.267404](https://doi.org/10.1103/PhysRevLett.109.267404).
- [106] G. M. Andolina, F. M. D. Pellegrino, V. Giovannetti, A. H. MacDonald and M. Polini, *Cavity quantum electrodynamics of strongly correlated electron systems: A no-go theorem for photon condensation*, Phys. Rev. B **100**, 121109 (2019), doi:[10.1103/PhysRevB.100.121109](https://doi.org/10.1103/PhysRevB.100.121109).
- [107] D. Guerci, P. Simon and C. Mora, *Superradiant phase transition in electronic systems and emergent topological phases*, arXiv:2005.09088 [cond-mat.mes-hall] (2020).
- [108] G. M. Andolina, F. M. D. Pellegrino, V. Giovannetti, A. H. MacDonald and M. Polini, *Theory of photon condensation in a spatially varying electromagnetic field*, Phys. Rev. B **102**, 125137 (2020), doi:[10.1103/PhysRevB.102.125137](https://doi.org/10.1103/PhysRevB.102.125137).
- [109] L. Mandel, *Sub-poissonian photon statistics in resonance fluorescence*, Opt. Lett. **4**(7), 205 (1979), doi:[10.1364/OL.4.000205](https://doi.org/10.1364/OL.4.000205).
- [110] J. J. Hopfield, *Theory of the contribution of excitons to the complex dielectric constant of crystals*, Phys. Rev. **112**, 1555 (1958), doi:[10.1103/PhysRev.112.1555](https://doi.org/10.1103/PhysRev.112.1555).
- [111] Y. Guo, R. M. Kroeze, V. D. Vaidya, J. Keeling and B. L. Lev, *Sign-changing photon-mediated atom interactions in multimode cavity quantum electrodynamics*, Phys. Rev. Lett. **122**, 193601 (2019), doi:[10.1103/PhysRevLett.122.193601](https://doi.org/10.1103/PhysRevLett.122.193601).
- [112] V. D. Vaidya, Y. Guo, R. M. Kroeze, K. E. Ballantine, A. J. Kollár, J. Keeling and B. L. Lev, *Tunable-range, photon-mediated atomic interactions in multimode cavity qed*, Phys. Rev. X **8**, 011002 (2018), doi:[10.1103/PhysRevX.8.011002](https://doi.org/10.1103/PhysRevX.8.011002).
- [113] M. A. Bastarrachea-Magnani, J. Thomsen, A. Camacho-Guardian and G. M. Bruun, *Polaritons in an electron gas—quasiparticles and landau effective interactions*, Atoms **9**(4), 81 (2021).
- [114] A. Camacho-Guardian, M. A. Bastarrachea-Magnani and G. M. Bruun, *Mediated interactions and photon bound states in an exciton-polariton mixture*, Phys. Rev. Lett. **126**(1), 017401 (2021).

- 
- [115] M. A. Masharin, V. A. Shahnazaryan, F. A. Benimetsky, D. N. Krizhanovskii, I. A. Shelykh, I. V. Iorsh, S. V. Makarov and A. K. Samusev, *Polaron-enhanced polariton nonlinearity in lead halide perovskites*, doi:[10.48550/ARXIV.2201.10265](https://doi.org/10.48550/ARXIV.2201.10265) (2022).
- [116] H. Deng, H. Haug and Y. Yamamoto, *Exciton-polariton bose-einstein condensation*, *Rev. Mod. Phys.* **82**, 1489 (2010), doi:[10.1103/RevModPhys.82.1489](https://doi.org/10.1103/RevModPhys.82.1489).